

TAILORING THE THIRD DIMENSION OF LAYERED DOUBLE HYDROXIDES

THESIS

Presented to the Graduate Council of
Texas State University-San Marcos
in Partial Fulfillment
of the Requirements

for the Degree

Master of SCIENCE

By

Jingfang Yu, B.E.

San Marcos, Texas
May 2013

TAILORING THE THIRD DIMENSION OF LAYERED DOUBLE HYDROXIDES

Committee Members Approved:

Luyi Sun, Chair

Benjamin R. Martin

Clois E. Powell

Approved:

J. Michael Willoughby
Dean of the Graduate College

COPYRIGHT

by

Jingfang Yu

2013

FAIR USE AND AUTHOR'S PERMISSION STATEMENT

Fair Use

This work is protected by the Copyright Laws of the United States (Public Law 94-553, section 107). Consistent with fair use as defined in the Copyright Laws, brief quotations from this material are allow with proper acknowledgment. Use of this material for financial gain without the author's express written permission is not allowed.

Duplication Permission

As the copyright holder of the work I, Jingfang Yu, refuse permission to copy in excess of the "Fair Use" exemption without my written permission.

ACKNOWLEDGEMENTS

I would like to thank my advisor, Dr. Luyi Sun for his support and encouragement in doing my exploration. And I would like to thank my committee members: Dr. Benjamin R. Martin and Dr. Clois E. Powell for their advice. In addition, I thank my group members: Johnathan E. Sims and Michael T. Spiegel, who helped me perform my experiments; as well as Dr. Fuchuan Ding, Jarett C. Martin, Haoran Chen, and Dr. Yan Li. Finally, I would like to thank my parents, Guosheng Yu and Guozhong Xu, for their huge support.

This research was partially sponsored by the Research Corporation for Science Advancement (Award No.: 19770), the U.S. Department of Agriculture (No.2011-38422-30803), the National Science Foundation (Partnerships for Research and Education in Materials, DMR-1205670), the Air Force Office of Scientific Research (award No. FA9550-12-1-0159), and the Welch Foundation.

This manuscript was submitted on April 8th 2013.

.

TABLE OF CONTENTS

	Page
ACKNOWLEDGEMENTS	v
LIST OF TABLES	viii
LIST OF FIGURES	ix
ABSTRACT.....	xi
 CHAPTER	
I. INTRODUCTION	1
1. Introduction of LDHs.....	1
2. Intercalation of LDHs	3
3. Exfoliation of LDHs	4
References	8
II. DIRECT SYNTHESIS OF LDH NANOSHEETS, INHIBIT THE THIRD DIMENSION GROWTH.....	17
1. Introduction.....	17
2. Experimental	18
2.1. Chemicals.....	18
2.2. Synthesis method	18
2.3. Characterization	19
3. Results and Discussion	19
4. Conclusions.....	34
References	36
III. IN SITU SYNTHESIS OF LDH/POLYELECTROLYTE INTERCALATION COMPOUNDS	38

1. Introduction.....	38
2. Experimental.....	39
2.1. Materials	39
2.2. Synthesis method	39
2.3. Characterization	40
3. Results and Discussion	40
4. Conclusions.....	53
References	54
IV. SUMMARY AND FUTURE WORK	57

LIST OF TABLES

Table	Page
1. XRD data for Mg/Al- LDH and polyelectrolyte intercalation compounds	44

LIST OF FIGURES

Table	Page
1. A typical structure of layered double hydroxide.....	1
2. X-ray patterns of MgAlCl-HTlc (a) and CuCoAl-HTlc (b).....	3
3. General process of exfoliating LDHs	5
4. Schematic of the growth of LDH inhibited in Z direction by formamide (not drawn to scale)	20
5. Digital photograph of as-prepared LDHs nanosheets in water	20
6. XRD pattern of titration synthesized Mg/Al-LDH	22
7. XRD patterns of: a) directly synthesized Mg/Al- LDH single-layer nanosheets in liquid phase. (b) pre-synthesized Mg/Al-LDH at a concentration of 0.2 g/mL in liquid phase. (c) directly synthesized two dimensional Mg/Al- LDH nanosheets restacked on silicon wafer after drying	23
8. TEM images of as-prepared Mg/Al-LDH single-layer nanosheets	24
9. SEM images of the prepared Mg/Al-LDH single-layer nanosheets	25
10. XRD patterns of Mg/Al-LDH nanosheets titration synthesized with different vol% of formamide compared with the original Mg/Al-LDH	26
11. Liquid phase XRD pattern of Mg/Al-LDH nanosheets titration synthesized with different vol% of formamide	27
12. Digital images (A) and the Tyndall effect (B) of Mg/Al-LDH nanosheets titration synthesized with different vol% of formamide from left to right: 100 vol%, 70 vol%, 50 vol%, 23 vol%, 10 vol%, 5 vol% and D.I. water	28
13. Mg/Al-LDH nanosheets synthesized with 5 vol% formamide	29
14. Mg/Al-LDH nanosheets synthesized with 10 vol% formamide	29

15. Mg/Al-LDH nanosheets synthesized with 50 vol% formamide	30
16. Mg/Al-LDH nanosheets synthesized with 70 vol% formamide	30
17. Mg/Al-LDH nanosheets synthesized with 100 vol% formamide	31
18. TEM images of aged Mg/Al-LDH nanosheets synthesized with 23 vol% formamide.	32
19. Digital photographs of as-prepared LDHs nanosheets in water (B) and aged as- prepared sample in 100% formamide(right after aging) (A).	33
20. SEM images of Mg/Al-LDH nanosheets synthesized with 100 vol% formamide after aging.....	34
21. XRD patterns of LDH/PSSS intercalation compounds with different weight ratios of PSSS	42
22. XRD patterns of LDH/PAAS intercalation compounds with different weight ratios of PAAS	43
23. IR spectra of LDH/PSSS intercalation compounds with different weight ratios of PSSS	45
24. IR spectra of LDH/PAAS intercalation compounds with different weight ratios of PAAS	46
25. TGA profile of LDH/PSSS intercalation compounds with different weight ratios of PSSS.	48
26. Derivative TGA profile of LDH/PSSS intercalation compounds with different weight ratios of PSSS.....	48
27. TGA profile of LDH/PAAS intercalation compounds with different weight ratios of PAAS	49
28. Derivative TGA profile of LDH/PAAS intercalation compounds with different weight ratios of PAAS	50
29. SEM images of the hydrothermally synthesized pristine LDH	51
30. SEM images of LDH/PSSS intercalation compounds with different weight ratios of PSSS.....	52
31. SEM images of LDH/PAAS intercalation compounds with different weight ratio of PAAS.....	53

ABSTRACT

TAILORING THE THIRD DIMENSION OF LAYERED DOUBLE HYDROXIDES

by

Jingfang Yu, B.E.

Texas State University-San Marcos

May 2013

SUPERVISING PROFESSOR: DR. LUYI SUN

Layered double hydroxides (LDHs) have attracted lots of attention in the research field for their controllable composition and gallery spacing. LDHs have been used as catalysts, anion exchange materials, fire retardants and in polymer nanocomposites. Exfoliating LDHs into single layers nanosheets, can make the most use of the layers. New physical properties under nanoscale make new inventions of multifunctional materials possible. Different approaches to delaminate LDHs were reviewed in this thesis. Yet, none of the reported methods to obtain 2-D LDHs nanosheets was efficient. Herein, we report a new methodology to directly synthesize LDHs nanosheets. Mg/Al-LDHs nanosheets were synthesized in the presence of 23% formamide via a titration method. Formamide was used as an inhibitor that prevents the growth of LDHs in the Z-direction. LDHs/polymer nanocomposites have been extensively studied. Various methods to prepare LDHs nanocomposites have been developed. In situ intercalation of polyelectrolytes into LDHs has been reported. However, the exclusion of CO₂ is a requirement during the process. Herein, we report a new approach to prepare

LDHs/polyelectrolyte intercalation compounds via an in situ intercalation method. The LDH was synthesized in the presence of a polyelectrolyte [poly(sodium 4-styrenesulfonate) (PSSS) or poly(acrylic acid, sodium) (PAAS)] by a urea hydrolysis method. Characterization data confirmed the successful intercalation. The intercalated polyelectrolytes turned to be more thermally stable as confirmed by the TGA data.

CHAPTER I

INTRODUCTION

1. Introduction of LDHs

In recent years, inorganic layered materials at nanoscale have aroused intensive interest in the application of new polymer nanocomposites,¹ ion exchanger,² photochemistry,³ and catalysis.⁴ Layered double hydroxides (LDHs), known as anion clays, are one of the most thoroughly studied layered materials.⁵ LDHs are comprised of positively charged metallic panel and interlayer anions. The general formula of LDHs is $[M^{2+}_{1-x}M^{3+}_x(OH)_2]^{x+}[A^{p-}_{x/p}]^{x+} \cdot mH_2O$ (see Figure 1), where M^{2+} and M^{3+} are a metallic bivalent cation and a metallic trivalent cation respectively and A^{n-} is the interlayer anion. X is the ratio of two metals which is subject to change to fit special requirements.

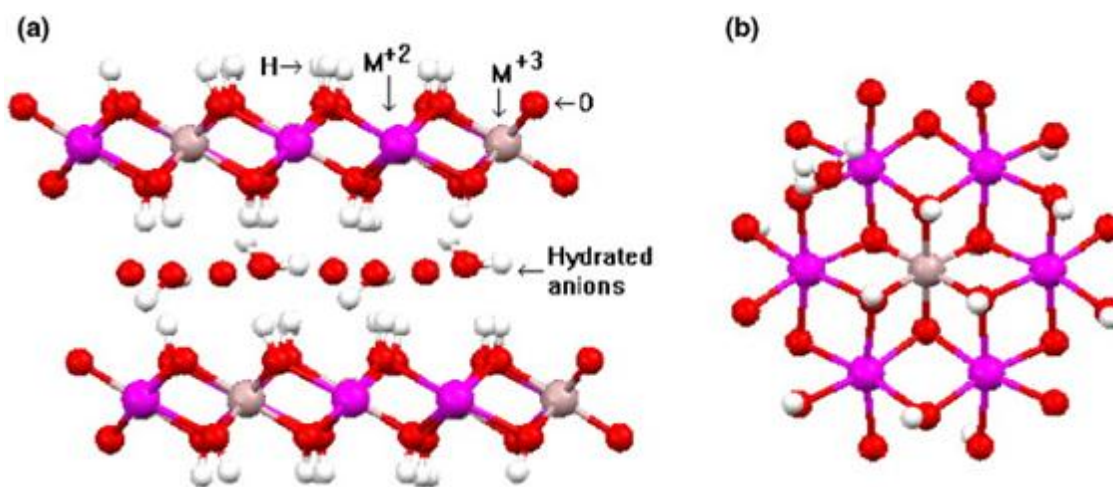


Figure 1. A typical structure of layered double hydroxide.⁶

Layered double hydroxides can be prepared through the co-precipitation of inorganic salts in basic solution at low or high supersaturation, hydrothermal synthesis, reconstruction and ion-exchange methods.⁵ Different advantages have been observed as a function of different methods of LDHs synthesis.

Co-precipitation method:⁵ Construction metal salts and base co-precipitate at supersaturate condition. There are two different methods based on operations: (1) Co-precipitation at high supersaturation and (2) Co-precipitation at low supersaturation. When using co-precipitation at high supersaturation, a solution containing M^{2+} and M^{3+} is added to a base solution which contains interlayer anions. The reaction is stopped when the set pH value is reached. Co-precipitation at low supersaturation, two solutions are mixed together drop by drop. Solution A contains construction metal cations and solution B contains counter anion and precipitation base.

Ion exchange method:⁵ The counter anions in LDHs can be ion exchanged. LDHs with different counter anions can be obtained through ion exchange.

Calcine recovery method:⁷ LDHs exhibit a unique memory effect. LDHs that contain interlayer CO_3^{2-} (most common) can decompose into metal oxides when calcined at 500 °C. The original structure can be recovered after the metal oxides are placed into basic solution containing the desired counter anion. In this way, one can obtain various LDHs.

Urea hydrolysis method:⁸ urea is neutral at low temperatures and hydrolyzes above 90 °C to render solution basic. The homogenous increasing of pH by urea hydrolysis allows to synthesis LDHs with high crystallinity and purity.

Microwave method:⁹ Microwave will heat the reaction system in a very energy efficient manner when compared to the conventional preparation methods. It shortens the reaction time.

Figure 2 shows the typical XRD patterns of hydrotalcite like compounds (HTlc).

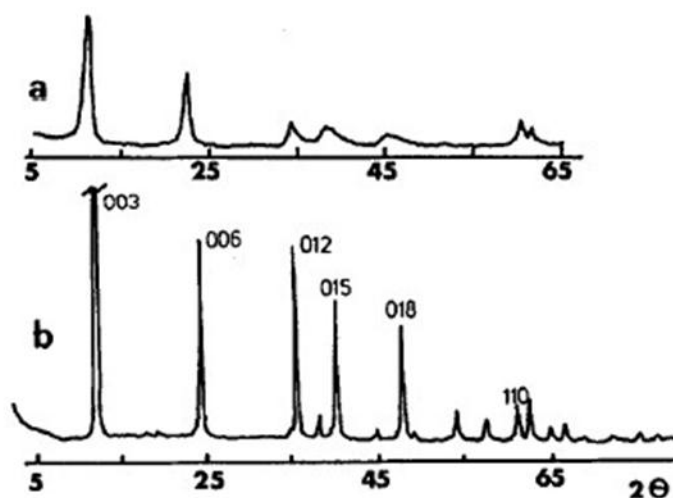


Figure 2. X-ray patterns of MgAlCl-HTlc (a) and CuCoAl-HTlc (b).⁵

2. Intercalation of LDHs

Recently, LDH/polymer interaction compounds have received a large amount of attention because of their superior thermal,¹⁰ mechanical, electrical, and chemical properties.¹¹ A wide range of anions can be intercalated into the galleries of LDHs,¹² among which, polyanions are the most intensively investigated. The approaches to achieve intercalation in LDHs including ion exchange method,⁵ secondary intercalation method,¹³ in situ intercalation method¹⁴ and calcination and reconstruction method,¹⁵ all of which have been well established. In situ intercalation of polyanions has been reported to be successful with poly(styrene sulfonate), poly(vinyl sulfonate), polyaspartate, poly(ethylene oxide) derivatives, and poly(acrylic acid),¹⁴ by the co-precipitation method.

In this thesis, we used the urea hydrolysis method under hydrothermal condition, which typically generates high crystallinity LDHs, to explore the potential in situ synthesis of LDH/polyelectrolyte intercalation compounds. The effect of the polyelectrolytes on guiding the growth of the layered materials in the Z direction was a prime focus.

3. Exfoliation of LDHs

LDHs have been used to prepare various functional materials, including catalysts, optical materials, and polymer nanocomposites.⁵ However, their usage is limited because the lamellar flakes of LDHs form stacks and bundles.¹¹ Exfoliating LDHs into individual layers (i.e., nanosheets) will maximize the utility of the layers by ensuring a high specific surface and aspect ratio. Such nanosheets can be used as building blocks for the fabrication of a wide variety of functional nanostructured materials.^{5, 16} One important example is the layer-by-layer assembly of nanosheets with appropriate counterparts through a wet process.¹⁶⁻¹⁷ Compared to other layered inorganic compounds, LDHs are difficult to exfoliate due to their high charge density on the layers.¹⁸ Complete exfoliation of LDHs optimizes properties of the resultant nanostructured materials and improves efficiency.

LDHs have high planar charge density, leading to strong electrostatic interactions between layers. Therefore, LDHs are difficult to be exfoliated except under some specific conditions. The exfoliation of LDHs was first achieved by intercalating anionic organic guests such as amino acids or surfactants into the interlayer of LDHs and agitated in certain solvents (Figure 3). Later, delamination of LDHs without intercalated organic species in gallery was achieved by using formamide as solvent which provides a faster

and more efficient approach to achieve the goal. Recently, more efficient LDHs exfoliation methods, laser ablation, have been developed, which takes several minutes to finish the delamination.

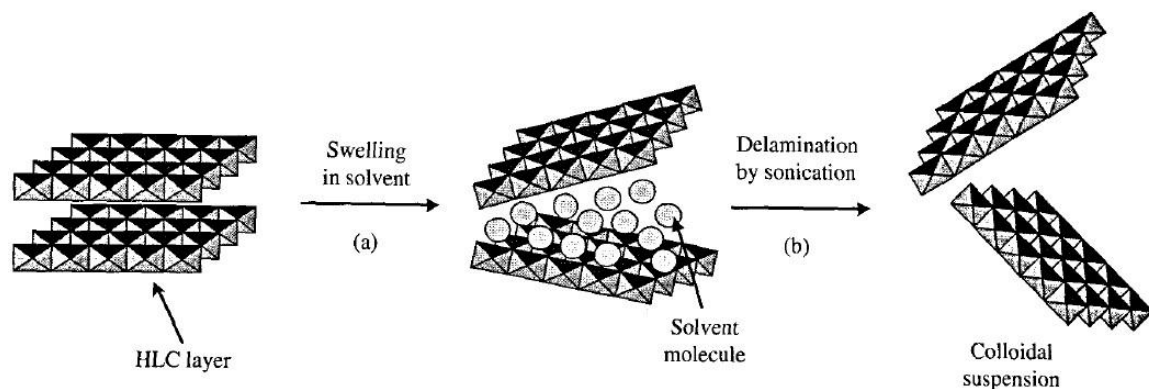


Figure 3. General process of exfoliating LDHs.²⁰

Representative exfoliation methods:

1) Exfoliation of LDHs in formamide

Hibino et al. reported²¹ the exfoliation of the pre-synthesized glycine intercalated LDHs in formamide. Approximately 0.03 g Mg/Al-Gly-LDHs was dispersed in 10 mL of formamide, which produced a colloid within a few minutes. Similar approaches have been reported by Ugur²² who successfully exfoliated Mg/Ga-LDHs. Li et al.¹⁶ reported the exfoliation of a well crystallized NO_3^- containing Mg/Al-LDHs delaminated in formamide. Liu et al.²³ prepared Co/Al-LDHs through ion exchange with NO_3^- that were exfoliated in formamide. A modified homogeneous precipitation method was used to prepare Ni/Fe- CO_3^{2-} -LDHs. Urea and triethanolamine (TEA) were used as the ammonia releasing reagent and chelating agent, respectively, to facilitate its exfoliation in formamide.²⁴ Mg/Al-LDHs could be exfoliated under ultrasonication treatment. Mg/Al-

NO_3 -LDHs synthesized by co-precipitation method under constant $\text{pH}=10.0$ at about 60°C was dispersed in formamide with concentrations of 1, 5, 10, 20 and 40 g L^{-1} . The dispersions were treated with an ultrasonic water bath in successive intervals of 30 min, until the turbidity of the dispersion approached a constant value.²⁵

2) Exfoliation of LDHs in several other solvents

Chen et al.²⁶ reported that $\text{Mg}_3/\text{Al-OH-C}_{12}\text{H}_{25}\text{SO}_4$ -LDHs could be exfoliated in a xylene solution of polyethylene grafted with maleic anhydride (PEG-MA). Chen et al.²⁶⁻²⁷ reported that an advanced exfoliation system prepared from a pre-synthesized $\text{Zn}_3\text{Al}(\text{OH})_8(\text{C}_{12}\text{H}_{25}\text{SO}_4)$ [named Zn/Al-DS] LDH was exfoliated by refluxing in 50 mL of xylene solution with a desired amount of LDPE with stirring under a N_2 atmosphere for 24 h. Jobbágy et al.²⁸ reported that 0.4 g pre-synthesized dodecyl-sulfate-intercalated Mg/Al-LDH could be delaminated in 2 mL CCl_4 or toluene in screw capped test tubes through a 30 min ultra-sonication with 2 h equilibrium time at room temperature. Adachi-Pagano et al.²⁹ evaluated the dispersion of $\text{Zn}_2/\text{Al-DS-LDH}$ in water, methanol, ethanol, propanol, and hexane under reflux conditions. Exfoliation occurred in butanol only at 120°C for 16 h. Up to 1.5 g L^{-1} of Zn/Al-DS-LDH in butanol could be dispersed.

Other solvents have been evaluated, including water,³⁰ sodium lactate solution,³¹ chloroform,³² dimethyl sulfoxide,³³ silane,³⁴ and N,N-dimethylformamide,³⁵ to facilitate the exfoliation process.

3) Direct exfoliation method

Only one direct exfoliation method is reported. Zn/Al, Co/Fe, Co/Al and Mg/Fe-LDHs are synthesized by two consecutive steps: (1) laser ablation of trivalent metal

target in de-ionized water at room temperature using a Q-switched Nd:Yttrium aluminum garnet laser; (2) the same laser ablation over a bivalent metal target in a previously prepared trivalent metallic colloid.³⁶ The synthesized LDHs were characterized to be nanosheets.

References

1. (a) Gilman, J. W., Flammability and thermal stability studies of polymer layered-silicate (clay) nanocomposites. *Applied Clay Science* **1999**, *15* (1–2), 31-49; (b) Carrado, K. A.; Xu, L., In Situ Synthesis of Polymer–Clay Nanocomposites from Silicate Gels. *Chemistry of Materials* **1998**, *10* (5), 1440-1445; (c) Fu, X.; Qutubuddin, S., Polymer–clay nanocomposites: exfoliation of organophilic montmorillonite nanolayers in polystyrene. *Polymer* **2001**, *42* (2), 807-813; (d) Akelah, A.; Moet, A., Polymer-clay nanocomposites: Free-radical grafting of polystyrene on to organophilic montmorillonite interlayers. *Journal of Materials Science* **1996**, *31* (13), 3589-3596; (e) Okada, A.; Usuki, A., The chemistry of polymer-clay hybrids. *Materials Science and Engineering: C* **1995**, *3* (2), 109-115; (f) Kuila, T.; Acharya, H.; Srivastava, S. K.; Bhowmick, A. K., Ethylene vinyl acetate/Mg-Al LDH nanocomposites by solution blending. *Polymer Composites* **2009**, *30* (4), 497-502; (g) Kafunkova, E.; Lang, K.; Kubat, P.; Klementova, M.; Mosinger, J.; Slouf, M.; Troutier-Thuilliez, A.-L.; Leroux, F.; Verney, V.; Taviot-Gueho, C., Porphyrin-layered double hydroxide/polymer composites as novel ecological photoactive surfaces. *Journal of Materials Chemistry* **2010**, *20* (42), 9423-9432; (h) Lv, S.; Zhou, W.; Miao, H.; Shi, W., Preparation and properties of polymer/LDH nanocomposite used for UV curing coatings. *Progress in Organic Coatings* **2009**, *65* (4), 450-456.
2. (a) Pérez, M. R.; Pavlovic, I.; Barriga, C.; Cornejo, J.; Hermosín, M. C.; Ulibarri, M. A., Uptake of Cu²⁺, Cd²⁺ and Pb²⁺ on Zn–Al layered double hydroxide intercalated with edta. *Applied Clay Science* **2006**, *32* (3–4), 245-251; (b) Prévot, V.; Forano, C.; Besse, J. P., Hybrid derivatives of layered double hydroxides. *Applied Clay Science* **2001**,

18 (1–2), 3–15; (c) Millange, F.; Walton, R. I.; Lei, L.; O'Hare, D., Efficient Separation of Terephthalate and Phthalate Anions by Selective Ion-Exchange Intercalation in the Layered Double Hydroxide $\text{Ca}_2\text{Al}(\text{OH})_6\cdot\text{NO}_3\cdot 2\text{H}_2\text{O}$. *Chemistry of Materials* **2000**, *12* (7), 1990–1994; (d) Dutta, P. K.; Puri, M., Anion exchange in lithium aluminate hydroxides. *The Journal of Physical Chemistry* **1989**, *93* (1), 376–381; (e) Nijs, H.; Clearfield, A.; Vansant, E. F., The intercalation of phenylphosphonic acid in layered double hydroxides. *Microporous and Mesoporous Materials* **1998**, *23* (1–2), 97–108; (f) Rives, V.; Angeles Ulibarri, M. a., Layered double hydroxides (LDH) intercalated with metal coordination compounds and oxometalates. *Coordination Chemistry Reviews* **1999**, *181* (1), 61–120; (g) Costantino, U.; Casciola, M.; Massinelli, L.; Nocchetti, M.; Vivani, R., Intercalation and grafting of hydrogen phosphates and phosphonates into synthetic hydrotalcites and a.c.-conductivity of the compounds thereby obtained. *Solid State Ionics* **1997**, *97* (1–4), 203–212; (h) Crepaldi, E. L. P., P. C.; Valim, J. B., Anion exchange in layered double hydroxides by surfactant salt formation. *J. Mater. Chem.* **2000**, *10*, 1337; (i) Itaya, K.; Chang, H. C.; Uchida, I., Anion-exchanged clay (hydrotalcite-like compounds) modified electrodes. *Inorganic Chemistry* **1987**, *26* (4), 624–626; (j) Liu, J.; Wang, F.; Gu, Z.; Xu, X., Styrene epoxidation over Ag- γ -ZrP catalyst prepared by ion-exchange. *Catalysis Communications* **2009**, *10* (6), 868–871; (k) Kullberg, L.; Clearfield, A., Mechanism of ion exchange in zirconium phosphates. 32. Thermodynamics of alkali metal ion exchange on crystalline .alpha.-zirconium phosphate. *The Journal of Physical Chemistry* **1981**, *85* (11), 1585–1589.

3. (a) Robins, D. S.; Dutta, P. K., Examination of Fatty Acid Exchanged Layered Double Hydroxides as Supports for Photochemical Assemblies. *Langmuir* **1996**, *12* (2),

402-408; (b) Nakajima, H.; Ishino, S.; Masuda, H.; Shimosaka, T.; Nakagama, T.; Hobo, T.; Uchiyama, K., Photochemical Immobilization of Protein on Inner Wall of Microchannel. *Chemistry Letters* **2005**, *34* (3), 358-359; (c) Tagaya, H.; Ogata, S.; Nakano, S.; Kadokawa, J.-I.; Karasu, M.; Chiba, K., Intercalation of Azo Compounds into Layered Aluminium Dihydrogentriphosphate and a Layered Double Hydroxide. *Journal of Inclusion Phenomena and Macrocyclic Chemistry* **1998**, *31* (3), 231-241; (d) Atienzar, P.; de Victoria-Rodriguez, M.; Juanes, O.; Rodriguez-Ubis, J. C.; Brunet, E.; Garcia, H., Layered [gamma]-zirconium phosphate as novel semiconductor for dye sensitized solar cells: Improvement of photovoltaic efficiency by intercalation of a ruthenium complex-viologen dyad. *Energy & Environmental Science* **2011**, *4* (11), 4718-4726; (e) Colon, J. L.; Yang, C. Y.; Clearfield, A.; Martin, C. R., Photophysics and photochemistry of tris(2,2'-bipyridyl)ruthenium(II) within the layered inorganic solid zirconium phosphate sulfophenylphosphonate. *The Journal of Physical Chemistry* **1990**, *94* (2), 874-882.

4. (a) Liu, J.; Wang, F.; Xu, X., Creation of a Monomeric Ag Species on the Surface of γ -ZrP as an Efficient Heterogeneous Catalyst for the Selective Oxidation of Cycloolefins. *Catalysis Letters* **2008**, *120* (1), 106-110; (b) Wang, F.; Liu, J.; Xu, X., Layered material [gamma]-ZrP supported platinum catalyst for liquid-phase reaction: a highly active and selective catalyst for hydrogenation of the nitro group in para-chloronitrobenzene. *Chemical Communications* **2008**, (17), 2040-2042; (c) W.T, R., Pulse microreactor examination of the vapor-phase aldol condensation of acetone. *Journal of Catalysis* **1980**, *63* (2), 295-306; (d) Drezdson, M. A., Synthesis of isopolymetalate-pillared hydrotalcite via organic-anion-pillared precursors. *Inorganic*

- Chemistry* **1988**, 27 (25), 4628-4632; (e) Le Gendre, P.; Jerome, F.; Bruneau, C.; H. Dixneuf, P., Stereoselective synthesis of a new optically active phosphinoacyloxazolidinone via enantioselective hydrogenation. *Chemical Communications* **1998**, (5), 533-534; (f) Choudary, B. M.; Lakshmi Kantam, M.; Venkat Reddy, C. R.; Koteswara Rao, K.; Figueras, F., The first example of Michael addition catalysed by modified Mg–Al hydrotalcite. *Journal of Molecular Catalysis A: Chemical* **1999**, 146 (1–2), 279-284; (g) Perez-Ramirez, J.; Mul, G.; Kapteijn, F.; Moulijn, J. A., investigation of the thermal decomposition of Co-Al hydrotalcite in different atmospheres. *Journal of Materials Chemistry* **2001**, 11 (3), 821-830; (h) S. Kumbhar, P., Modified Mg-Al hydrotalcite: a highly active heterogeneous base catalyst for cyanoethylation of alcohols. *Chemical Communications* **1998**, (10), 1091-1092.
5. Cavani, F.; TrifirÃ², F.; Vaccari, A., Hydrotalcite-type anionic clays: Preparation, properties and applications. *Catalysis Today* **1991**, 11 (2), 173-301.
 6. Ma, R.; Liu, Z.; Li, L.; Iyi, N.; Sasaki, T., Exfoliating layered double hydroxides in formamide: a method to obtain positively charged nanosheets. *Journal of Materials Chemistry* **2006**, 16 (39), 3809-3813.
 7. Lv, L.; Sun, P.; Wang, Y.; Du, H.; Gu, T., Phosphate Removal and Recovery with Calcined Layered Double Hydroxides as an Adsorbent. *Phosphorus, Sulfur, and Silicon and the Related Elements* **2008**, 183 (2-3), 519-526.
 8. Adachi-Pagano, M.; Forano, C.; Besse, J.-P., Synthesis of Al-rich hydrotalcite-like compounds by using the urea hydrolysis reaction-control of size and morphology. *Journal of Materials Chemistry* **2003**, 13 (8), 1988-1993.

9. Hussein, M. Z. B.; Zainal, Z.; Ming, C. Y., Microwave-assisted synthesis of Zn-Al-layered double hydroxide-sodium dodecyl sulfate nanocomposite. *Journal of Materials Science Letters* **2000**, *19* (10), 879-883.
10. Kim, D. W.; Blumstein, A.; Tripathy, S. K., Nanocomposite Films Derived from Exfoliated Functional Aluminosilicate through Electrostatic Layer-by-Layer Assembly. *Chemistry of Materials* **2001**, *13* (5), 1916-1922.
11. Huang, S.; Peng, H.; Tjiu, W. W.; Yang, Z.; Zhu, H.; Tang, T.; Liu, T., Assembling Exfoliated Layered Double Hydroxide (LDH) Nanosheet/Carbon Nanotube (CNT) Hybrids via Electrostatic Force and Fabricating Nylon Nanocomposites. *The Journal of Physical Chemistry B* **2010**, *114* (50), 16766-16772.
12. Khan, A. I.; O'Hare, D., Intercalation chemistry of layered double hydroxides: recent developments and applications. *Journal of Materials Chemistry* **2002**, *12* (11), 3191-3198.
13. He, J.; Wei, M.; Li, B.; Kang, Y.; Evans, D.; Duan, X., Preparation of Layered Double Hydroxides. In *Layered Double Hydroxides*, Duan, X.; Evans, D., Eds. Springer Berlin Heidelberg: **2006**, Vol. 119, p 108.
14. Costa, F.; Saphiannikova, M.; Wagenknecht, U.; Heinrich, G., Layered Double Hydroxide Based Polymer Nanocomposites. In *Wax Crystal Control · Nanocomposites · Stimuli-Responsive Polymers*, Springer Berlin Heidelberg: **2008**, Vol. 210, pp 101-168.

15. He, J.; Wei, M.; Li, B.; Kang, Y.; Evans, D.; Duan, X., Preparation of Layered Double Hydroxides. In *Layered Double Hydroxides*, Duan, X.; Evans, D., Eds. Springer Berlin Heidelberg: **2006**, Vol. 119, p 107.
16. Li, L.; Ma, R.; Ebina, Y.; Iyi, N.; Sasaki, T., Positively Charged Nanosheets Derived via Total Delamination of Layered Double Hydroxides. *Chemistry of Materials* **2005**, *17* (17), 4386-4391.
17. Okamoto, K.; Tamura, K.; Takahashi, M.; Yamagishi, A., Preparation of a clay-metal complex hybrid film by the Langmuir-Blodgett method and its application as an electrode modifier. *Colloids and Surfaces A: Physicochemical and Engineering Aspects* **2000**, *169* (1-3), 241-249.
18. Li, B.; Hu, Y.; Zhang, R.; Chen, Z.; Fan, W., Preparation of the poly(vinyl alcohol)/layered double hydroxide nanocomposite. *Materials Research Bulletin* **2003**, *38* (11-12), 1567-1572.
19. Hou, W.; Kang, L.; Sun, R.; Liu, Z.-H., Exfoliation of layered double hydroxides by an electrostatic repulsion in aqueous solution. *Colloids and Surfaces A: Physicochemical and Engineering Aspects* **2008**, *312* (2-3), 92-98.
20. Hidalgo, J. M.; Jimenez, S.; Chen, C.; Sarmiento, M.; Ruiz, J.; Rafael, Formation of Stable Nanolayers of Meixnerite via a Combined Delamination-Ion Exchange Process. *Journal of Nanoscience and Nanotechnology* **2010**, *10* (10), 6562-6566.
21. Hibino, T.; Jones, W., New approach to the delamination of layered double hydroxides. *Journal of Materials Chemistry* **2001**, *11* (5), 1321-1323.

22. Ugur, U., Short-time hydrothermal synthesis and delamination of ion exchangeable Mg/Ga layered double hydroxides. *Journal of Solid State Chemistry* **2007**, *180* (9), 2525-2533.
23. Liu, Z.; Ma, R.; Osada, M.; Iyi, N.; Ebina, Y.; Takada, K.; Sasaki, T., Synthesis, Anion Exchange, and Delamination of Co-Al Layered Double Hydroxide. Assembly of the Exfoliated Nanosheet/Polyanion Composite Films and Magneto-Optical Studies. *Journal of the American Chemical Society* **2006**, *128* (14), 4872-4880.
24. Abellan, G.; Coronado, E.; Marti-Gastaldo, C.; Pinilla-Cienfuegos, E.; Ribera, A., Hexagonal nanosheets from the exfoliation of Ni²⁺-Fe³⁺ LDHs: a route towards layered multifunctional materials. *Journal of Materials Chemistry* **2010**, *20* (35), 7451-7455.
25. Wu, Q.; Olafsen, A.; Vistad, O. B.; Roots, J.; Norby, P., Delamination and restacking of a layered double hydroxide with nitrate as counter anion. *Journal of Materials Chemistry* **2005**, *15* (44), 4695-4700.
26. Chen, W.; Qu, B., Structural Characteristics and Thermal Properties of PE-g-MA/MgAl-LDH Exfoliation Nanocomposites Synthesized by Solution Intercalation. *Chemistry of Materials* **2003**, *15* (16), 3208-3213.
27. Chen, W.; Feng, L.; Qu, B., Preparation of Nanocomposites by Exfoliation of ZnAl Layered Double Hydroxides in Nonpolar LLDPE Solution. *Chemistry of Materials* **2004**, *16* (3), 368-370.

28. JobbÁgy, M. Ì. a.; Regazzoni, A. E., Delamination and restacking of hybrid layered double hydroxides assessed by in situ XRD. *Journal of Colloid and Interface Science* **2004**, 275 (1), 345-348.
29. Adachi-Pagano, M.; Forano, C.; Besse, J.-P., Delamination of layered double hydroxides by use of surfactants. *Chemical Communications* **2000**, (1), 91-92.
30. Hibino, T.; Kobayashi, M., Delamination of layered double hydroxides in water. *Journal of Materials Chemistry* **2005**, 15 (6), 653-656.
31. k. Okudaira, Y. K., T. Isobe, A. Nakajima, K. Okada Preparation of Lactate/Layered Double Hydroxide (LDH) Composites by Reconstruction Method and Behavior of Delamination. *J. Jpn. Soc. Colour Mater.* **2011**, 84 (1), 2-6.
32. Kottegoda, N. S.; Jones, W., Preparation and Characterisation of Li-Al-glycine Layered Double Hydroxides (LDHs)-Polymer Nanocomposites. *Macromolecular Symposia* **2005**, 222 (1), 65-72.
33. Zhao, Y.; Yang, W.; Xue, Y.; Wang, X.; Lin, T., Partial exfoliation of layered double hydroxides in DMSO: a route to transparent polymer nanocomposites. *Journal of Materials Chemistry* **2011**, 21 (13), 4869-4874.
34. Ding, P.; Qu, B.; Shi, L.; Ge, C.; Yang, H., Inorganic template directed assembly of dendritic LDH nanostructures and their properties of morphological preservation and facile exfoliation. *Materials Letters* **2008**, 62 (23), 3815-3817.

35. Gordijo, C. R.; Leopoldo Constantino, V. R.; de Oliveira Silva, D., Evidences for decarbonation and exfoliation of layered double hydroxide in N,N-dimethylformamide–ethanol solvent mixture. *Journal of Solid State Chemistry* **2007**, *180* (7), 1967-1976.
36. Hur, T., New approach to the synthesis of layered double hydroxides and associated ultrathin nanosheets in de-ionized water by laser ablation. *J. Appl. Phys.* **2010**, *108* (11), 114312.

CHAPTER II

DIRECT SYNTHESIS OF LDH NANOSHEETS, INHIBIT THE THIRD DIMENSION GROWTH

1. Introduction

2D nanosheets, such as graphene and inorganic nanosheets have been extensively investigated during the past two decades due to their extraordinary dielectric properties,¹ super electrical conducting properties,² catalyst³ and so on. 2D nanosheets based nanocomposites is one of the most extensively studied areas. Methods⁴ to obtain single-layer nanosheets have been developed. Cost effective production of nanosheets remains an attractive goal. While many approaches to synthesize nanosheets have been investigated, exfoliation of the pre-formed layered compounds into continuous phases, which takes multiple steps, is the preferred method. For example, the prevalent approach to exfoliate layered double hydroxides (LDHs) consists of two steps: the first step is to intercalate LDH with large size surfactants/ organic molecules or swell LDH in certain solvent. The second step is to exfoliate the modified LDHs through sonication or mechanical agitation into the continuous phase. However, those exfoliation processes are complicated, time consuming^{4d, 5} and are not productive. In the best case, 0.1 g of Co/Al-LDH is delaminated in 100 cm³ formamide.⁵ It is imperative that a facile, greener, and productive approach to synthesize LDH single layer must be developed.

Because of their tunable chemical compositions and perfect 2-D morphology with a molecular thickness, LDH single layer nanosheets is considered as one of the most ideal systems that serve as a model for the physical and chemical research of nanostructured 2-D materials. Exploration of the direct synthesis of magnesium and aluminum LDHs nanosheets by using formamide molecules as inhibitors to suppress the growth in the third dimension (Z direction) is the focus of this work. Formamide has been widely used as the exfoliating solvent to for different LDHs.⁶ The carbonyl functionality of formamide has a strong interaction with the surface of LDH. However, the nitrogen in the -NH₂ functionality does not form a strong interaction with the interlayer counter anions, which ultimately weakens the interlayer attraction.⁶ Thus, formamide as the inhibitor to direct synthesis of LDH nanosheets was employed.

2. Experimental

2.1 Chemicals

Mg(NO₃)₂•6H₂O(98%), Co(NO₃)₂•6H₂O(98%-102%), and formamide(99%) were bought from Alfa Aesar Co.. Al(NO₃)₃ •9H₂O (99%) was purchased from Acros Organics Co.. Sodium hydroxide pellets were obtained from Macron Co.. All chemicals were used as received without further purification.

2.2 Synthesis method

We modified the traditional titration method with an aim to directly synthesize single-layer magnesium/aluminum LDHs (Mg/Al-LDH) by adding a predetermined amount of formamide as the inhibitor. Solution A is composed of Mg(NO₃)₂ and Al(NO₃)₃ (the total metal salts concentration is 0.05 M and Mg²⁺/Al³⁺=4:1 molar ratio.) which is added at a flow rate of ca. 1 mL/min to a solution of NaCl (Al³⁺/Cl⁻ = 1) containing 23 vol%

formamide at 80 °C in an oil bath. The mixture is maintained at pH approximately 10 throughout the experiment by simultaneously adding solution B which is 0.25 M sodium hydroxide. Both the mixing and reaction processes were carried out with vigorous magnetic stirring. After the addition of metal salts solution was finished, the prepared sample was centrifuged at 28000 G force and washed with deionized water. The process was repeated three times. Single-layer LDH nanosheets dispersed in water was recovered. A control sample of regular layered Mg/Al-LDH was prepared under the same conditions without adding formamide.

2.3 Characterization

The products were characterized by X-ray diffraction (Bruker D8 with Cu K α radiation, $\lambda = 1.5406 \text{ \AA}$, 40 kV, 40 mA), JEOL 4000EX at 400 kV for TEM imaging and SAED; Helios NanoLab 400 Dual Beam from FEI for SEM imaging.

3. Results and Discussion

Mg/Al-LDH single-layer nanosheets

Formamide forms a strong interaction with LDH sheets surface. The direct synthesis of LDH nanosheets in the presence of formamide is expected to have formamide molecules adhering to the synthesized LDH sheets surface during the sheet growth. And the interactions between the layers and anions will be hindered by the formamide molecular because of its high dielectric constant. This will limit the growth of the sheets

in the X-Y plane, without stacking of the layers (Figure 4).

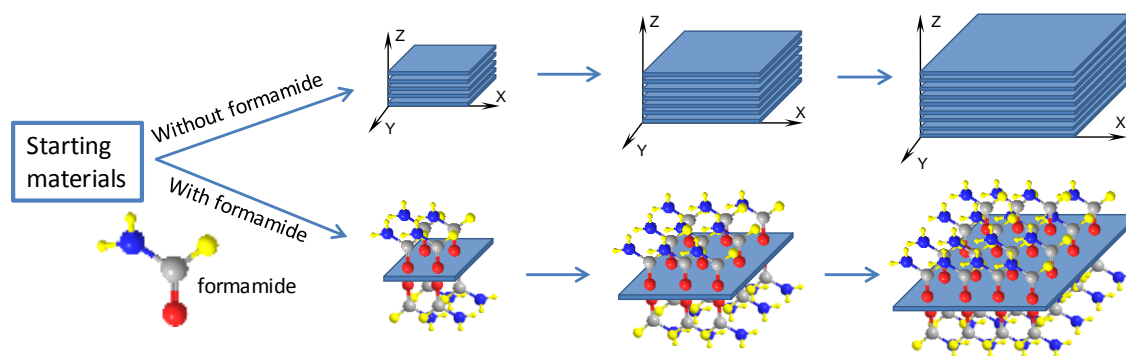


Figure 4. Schematic of the growth of LDH inhibited in Z direction by formamide (not drawn to scale).

A white transparent colloidal solution was obtained after dispersing the centrifuged sample into water. The Tyndall effect was clearly observed (Figure 5), indicating the presence of nanoscaled materials.



Figure 5. Digital photograph of as-prepared LDHs nanosheets in water.

Three samples were prepared for XRD characterization: sample A was a thin liquid layer of the suspension containing Mg/Al-LDH single- layer nanosheets in water, which was cast on a silicon wafer and covered by a Mylar® film; sample B was a thin layer of water suspension containing pre-synthesized Mg/Al-LDH (synthesized by the same

method for (A) without formamid) in water, which was cast on a silicon wafer and covered by a Mylar® film; sample C was a drop of MgAl-LDH single-layer nanosheets suspension in water which was cast and dried in air on a silicon wafer.

For the purpose of comparison, Mg/Al-LDH synthesized under the same condition was prepared. Figure 6 shows the XRD patterns of the LDH control sample, exhibiting characteristic sharp and symmetric peaks at low angular region.⁷

Figure 7a shows the XRD pattern of the sample: A. Mg/Al-LDH single-layer nanosheets suspended in water does not show any peak corresponding to a layered structure. This indicates that the synthesized Mg/Al-LDH single-layer nanosheets are probably not associated in stacked multi-layers. The diffraction peak at around 25.8° is from the Mylar® film, which covers the liquid sample. In contrast, Figure 7b shows the XRD pattern of an aqueous suspension of a pre-synthesized Mg/Al-LDH at a similar concentration. A diffraction peak at 11.57° , which corresponds to the stacked layered structure of LDH, is observed. Figure 7c shows the XRD pattern of the re-stacking the synthesized the LDH single-layer nanosheets dried on a silicon wafer. After precipitation and drying, the single-layer nanosheets re-stacked to form a layered structure, as evidenced by a 003 plane diffraction peak at 11.02° (8.0 \AA) and a 006 plane diffraction peak at 22.39° (4.0 \AA), which is similar to the control LDH.

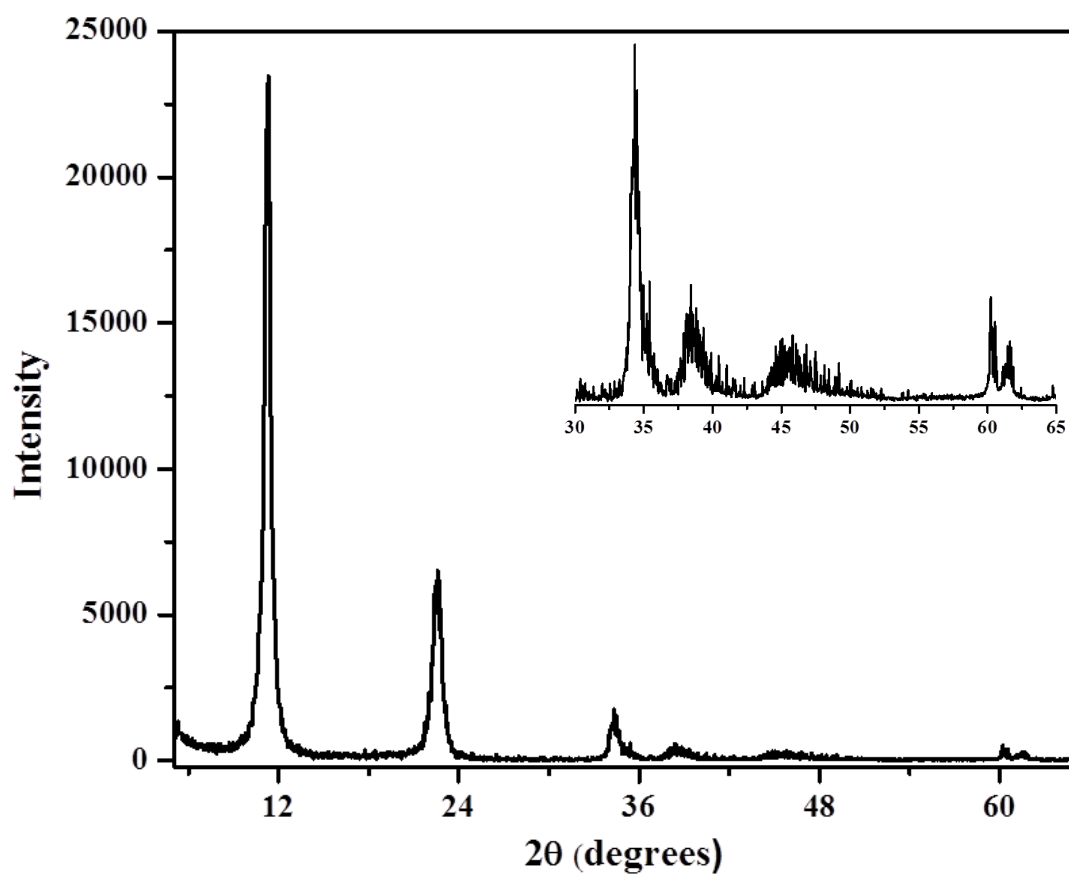


Figure 6. XRD pattern of titration synthesized Mg/Al-LDH.

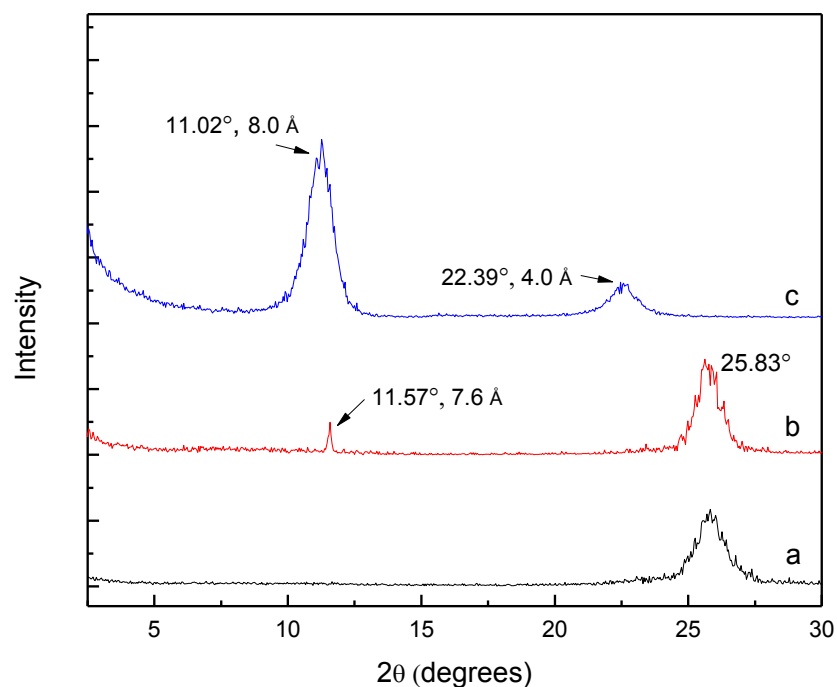


Figure 7. XRD patterns of: (a) directly synthesized Mg/Al- LDH single-layer nanosheets in liquid phase. (b) pre-synthesized Mg/Al-LDH at a concentration of 0.2 g/mL in liquid phase. (c) directly synthesized two dimensional Mg/Al- LDH nanosheets restacked on silicon wafer after drying.

The morphology and size dimension of the as-prepared nanosheets were examined by TEM and SEM. Figure 8 shows a representative TEM image of the synthesized LDH single-layer nanosheets. The hexagon shaped nanosheets suggest that the single-layer LDH nanosheets are moderately crystallized. The sheets exhibit narrow size distribution of approximately 20-100 nm in diameter. The High Resolution TEM image suggests that the single sheets morphology was prepared.

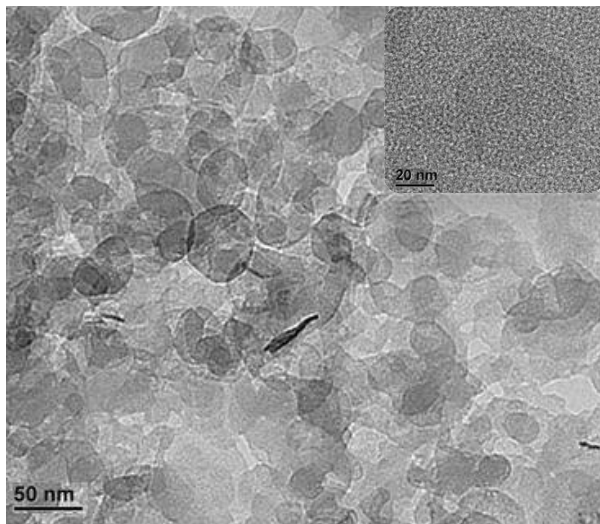


Figure 8. TEM images of as-prepared Mg/Al-LDH single-layer nanosheets.

The sample was also characterized using SEM. A liquid sample was cast on a silicon wafer and dried overnight. Figure 9 shows the representative morphology under SEM. The original LDH layered structure was not observed. Instead, a film-like morphology formed.

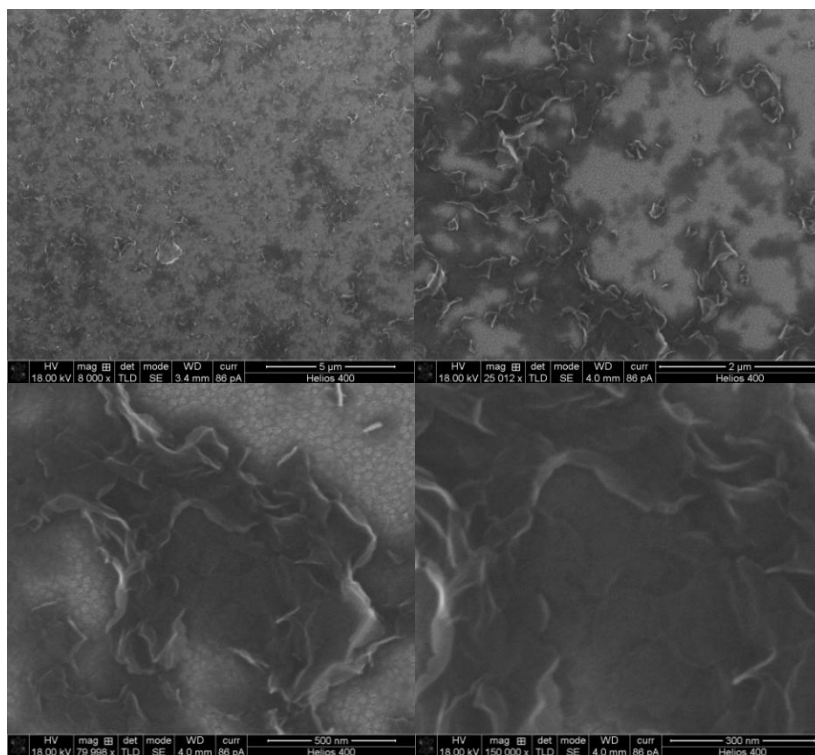


Figure 9. SEM images of the prepared Mg/Al-LDH single-layer nanosheets.

Influence of formamide

In order to investigate the effect of formamide in the growth of LDH, samples of Mg/Al –LDH nanosheets synthesized using the same method with various concentrations (vol%) of formamide were obtained. The total metal ion concentration was selected at 0.05 M to obtain pure LDH nanosheets. Drying the samples at low temperature (60 °C) for half an hour on silicon wafer resulted in similar restacking behavior of titration synthesized Mg/Al –LDH with 5, 10, 23, 50, 70, and 100 vol% formamide. From the X-ray diffraction patterns (figure 10), one can see that diffraction peaks of restacked Mg/Al –LDH nanosheets are broader and less symmetric than the control Mg/Al –LDH sample titration synthesized without formamide. This should be the result of a less ordered structure from the nanosheet restacking. Their d-spacing is similar. Since the formamide

molecule is smaller than NO_3^- and CO_3^{2-} ions,⁸ the d-spacing of the dried samples should be smaller than the original Mg/Al-LDH synthesized without formamide. If the water is not removed during the drying process, the interlayer distance should be slightly larger than the pristine Mg/Al-LDH.

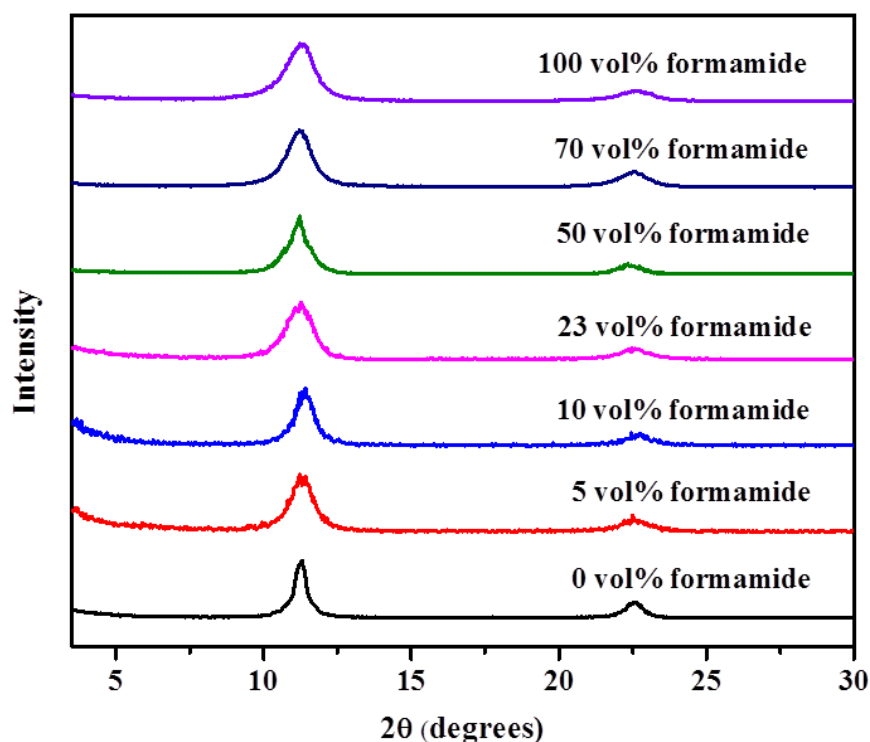


Figure 10. XRD patterns of Mg/Al-LDH nanosheets titration synthesized with different vol% of formamide compared with the original Mg/Al-LDH.

A series of liquid phase X-ray diffraction characterizations of the Mg/Al-LDH nanosheets titration synthesized with various vol% of formamide were conducted. In the liquid phase XRD patterns (Figure 11), the peaks in the low angular region of the pristine layered double hydroxide disappeared. A peak at ca. 25.8° appears from the diffraction of the Mylar® film which covers the liquid sample. The disappearance of the peaks in the low angular region suggests that no discernible layered structure can be detected.

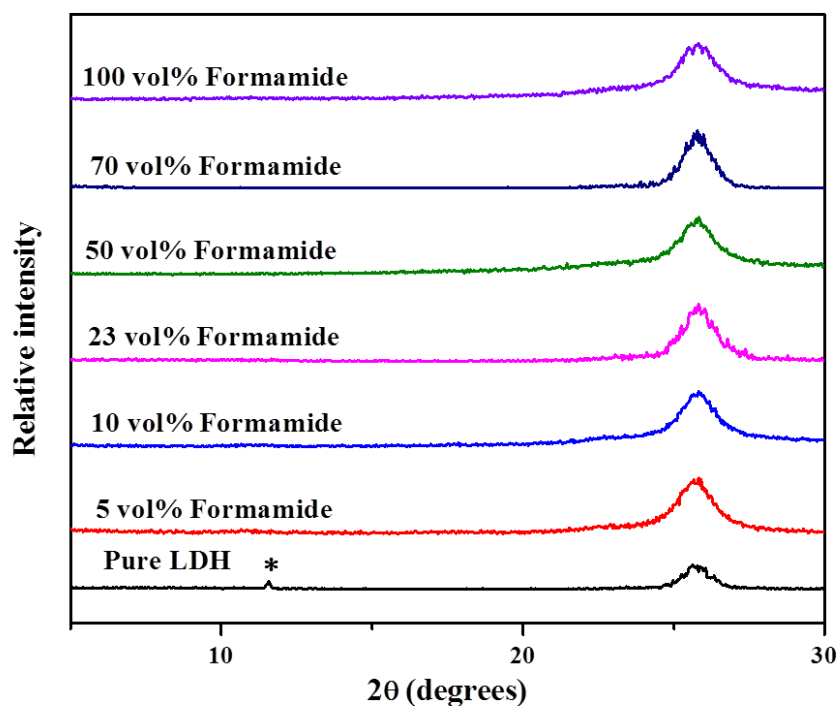


Figure 11. Liquid phase XRD pattern of Mg/Al-LDH nanosheets titration synthesized with different vol% of formamide.

Figure 12(A) shows the digital image of Mg/Al-LDH nanosheets synthesized with 5, 10, 23, 50, 70, and 100 vol% of formamide and deionized water (D.I. water) and their Tyndall effect under the shining of a green laser beam. With the increasing amount of formamide used in the synthesis process, the concentrations of Mg/Al-LDH nanosheets in D.I. water solution tend to be decreasing. All samples prepared with different volume percentages of formamide form a stable translucent suspension. They all show Tyndall effect as shown in Figure 12 (B).

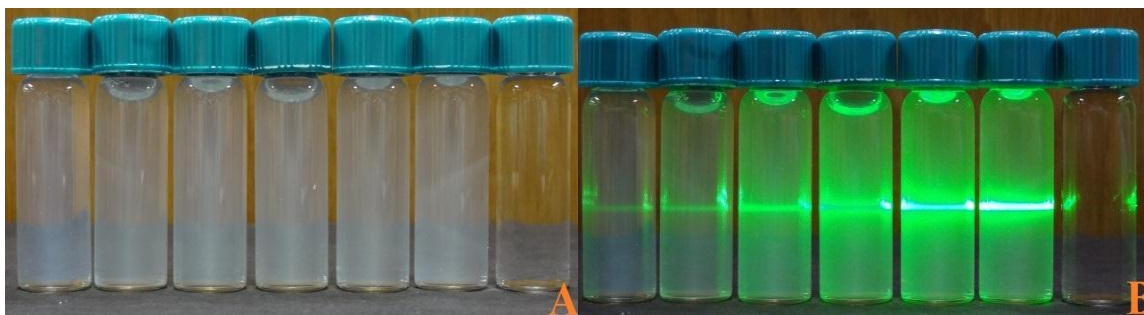


Figure 12. Digital images (A) and the Tyndall effect (B) of Mg/Al-LDH nanosheets titration synthesized with different vol% of formamide from left to right: 100 vol%, 70 vol%, 50 vol%, 23 vol%, 10 vol%, 5 vol%, and D.I water.

Transmission electron microscopy is also used to determine the difference between these samples. **Figures 13** through **16** shows the representative TEM images of the LDH nanosheets synthesized with different volume ratios of formamide with a fixed total metal ion concentration at 0.05M. Increasing the amount of formamide added to the synthesis, resulted in producing LDH with less defined crystallinity. At the extreme case, in which the LDH compound was synthesized in 100 vol% of formamide appeared to have virtually no hexagon shaped LDH structures in Figure 17. A possible reason might be because the large amount of formamide can form a micelle like structure and block the growth of LDH on Z and Y directions. The XRD pattern (Figure 10) and TEM images of LDH synthesized with low amounts of formamide indicates good crystallinity and are similar to pristine LDH. In order to synthesis LDH nanosheets with both good crystallinity and fewer layers, the LDH nanosheets synthesized with 23 % of formamide was chosen in the latter studies.

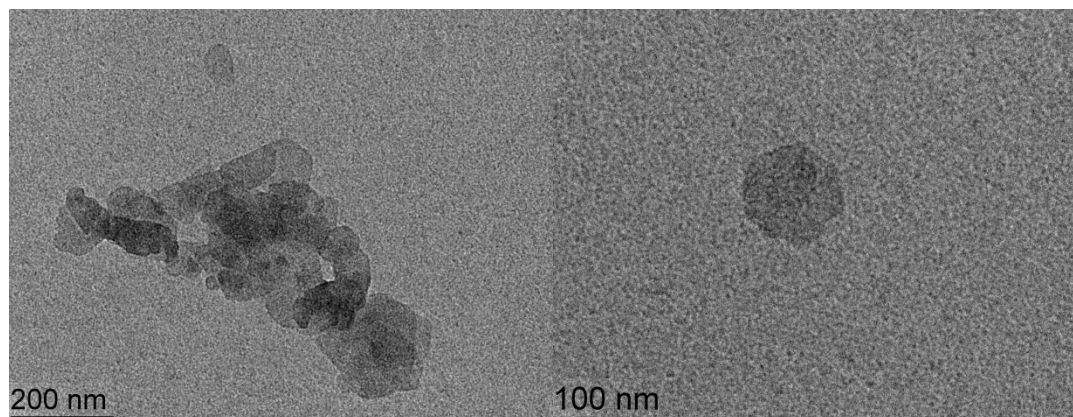


Figure 13. Mg/Al-LDH nanosheets synthesized with 5 vol% formamide.

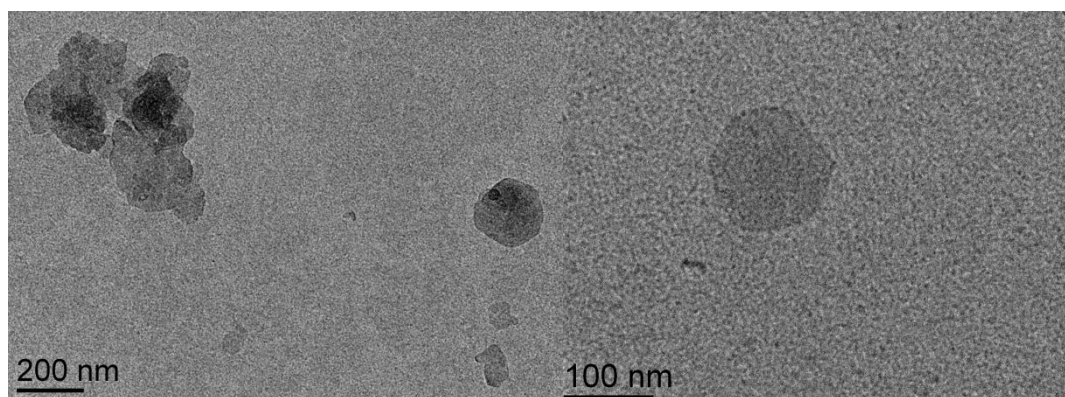


Figure 14. Mg/Al-LDH nanosheets synthesized with 10 vol% formamide.

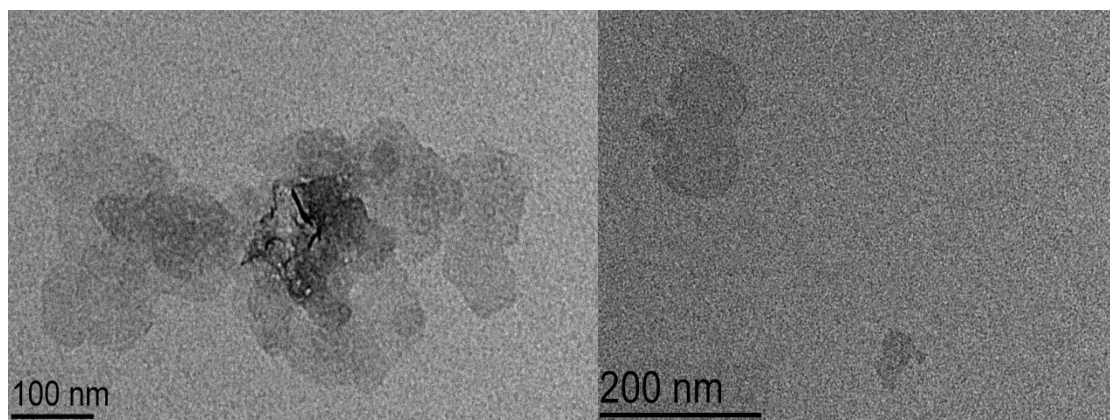


Figure 15. Mg/Al-LDH nanosheets synthesized with 50 vol% formamide.

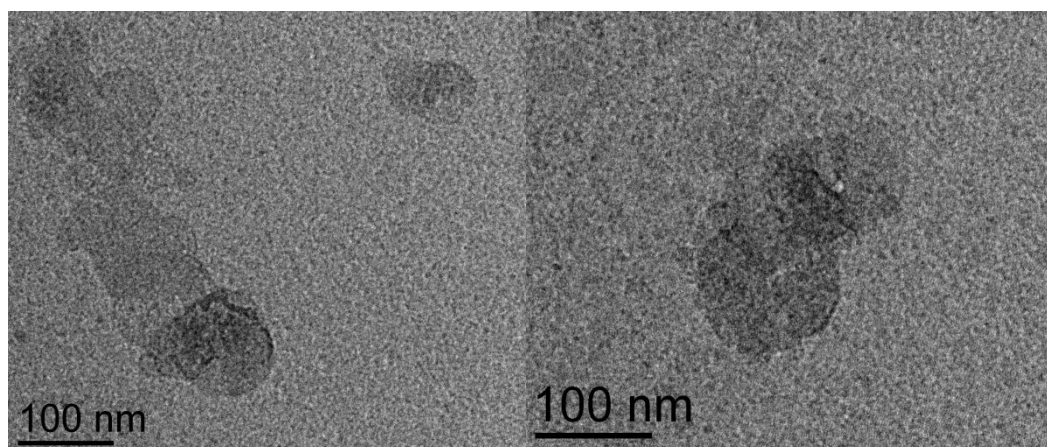


Figure 16. Mg/Al-LDH nanosheets synthesized with 70 vol% formamide.

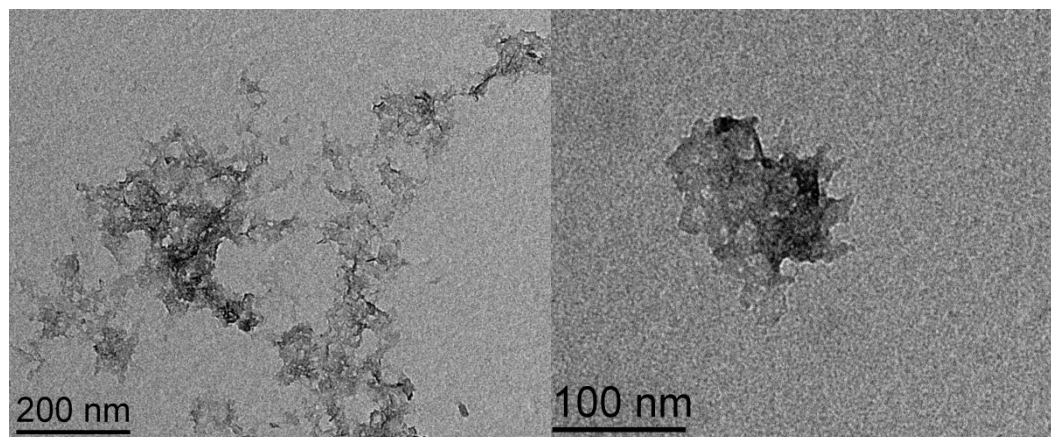


Figure 17. Mg/Al-LDH nanosheets synthesized with 100 vol% formamide.

Influence of aging

The Mg/Al-LDH nanosheets synthesized with 23 vol% formamide were not well crystallized as shown in the TEM images (Figure 8). Aging has been proven to be effective in assisting the crystallization of LDH.⁹ Two samples of Mg/Al-LDH nanosheets synthesized with 23 and 100 vol% formamide were aged for 18 hours at 80 °C. In Figure 18, the aged LDH nanosheets synthesized with 23 vol% formamide showed lower crystallinity than the un-aged sample. This is probably owing to the slow hydrolysis of formamide in the presence of sodium hydroxide residue into ammonium and formate.¹⁰ The hydrolysis of formamide destabilized the LDH nanosheets, which started to restack to form layered structure. Another experiment was conducted to verify this effect. The same method was applied as stated in the experiment section part except formamide was used as the solvent without water. Sodium hydroxide solid was dissolved in 100% formamide to prepare solution B. The metal salts were dissolved in 100% formamide to make solution A. Sodium chloride solid was dissolved in 100 % formamide prior to reaction in a three neck flask. After the reaction, half of the sample was subjected

to washing and the aggregates after washing was re-dispersion in water; the other half of the sample was preheated in an oven to 80 °C and aged for a day. A significant difference between the aged and un-aged samples can be observed (Figure 19 (A)). The aged sample formed discernible crystals and slowly precipitated out while the un-aged sample formed a transparent stable suspension as demonstrated by the Tyndall effect (Figure 19 (B)). The discernible crystals formed in the aged sample are the product of the hydrolysis of formamide (as is shown in Figure 16 B) which can be easily dissolved in water.

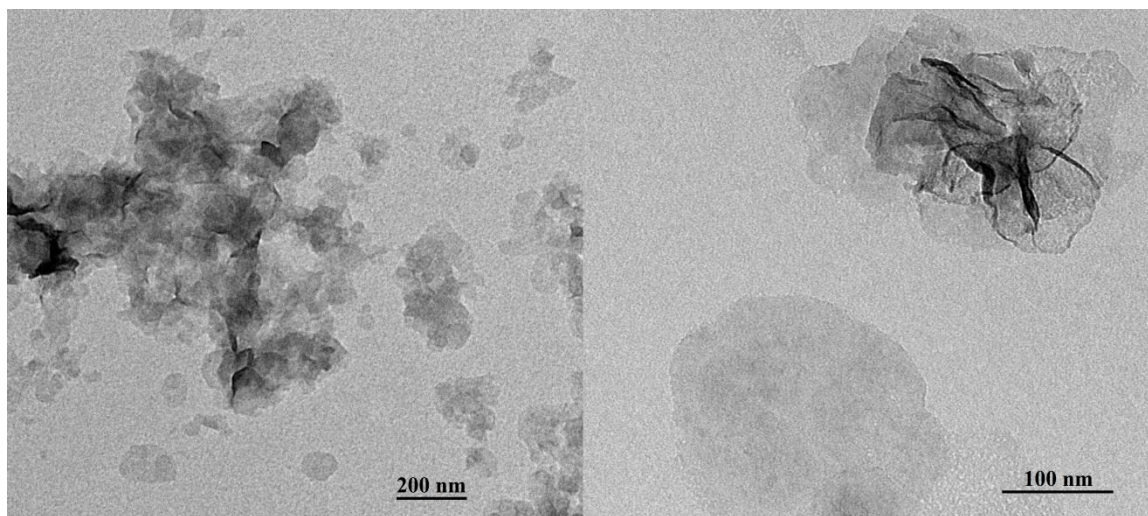


Figure 18. TEM images of aged Mg/Al-LDH nanosheets synthesized with 23 vol% formamide.

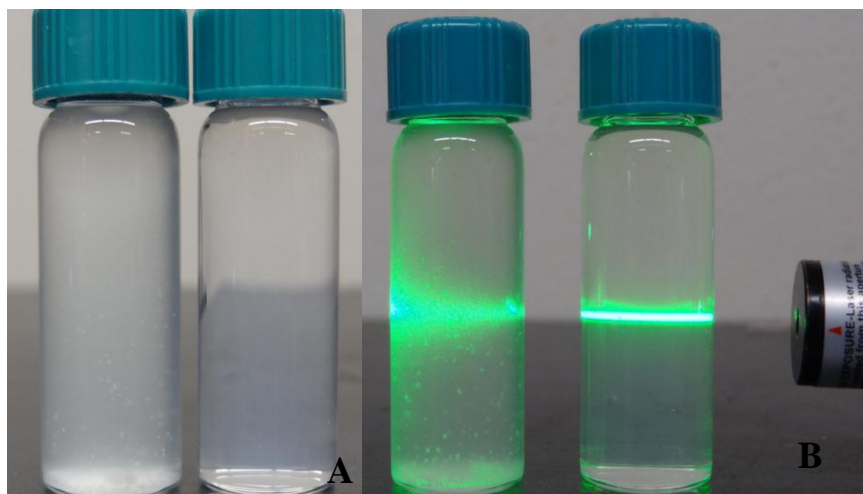


Figure 19. Digital photographs of as-prepared LDHs nanosheets in water (B) and aged as-prepared sample in 100% formamide(right after aging) (A).

Scanning electron microscopy was employed to observe the morphology of the aged sample synthesized in 100 vol% formamide (figure 20). After aging, the sheet-like morphology evolved to rosette-like LDH clusters. The SEM images indicate that aging improves the crystallinity of the synthesized nanosheets. The particle size increased from dozens of nanometer to several microns. In other words, the effect of formamide as an inhibitor during the synthesis of LDH nanosheets has been mitigated because of the aging. Formamide hydrolysed into ammonia and formate in a strongly basic environment. Probably, the LDH nanosheets would no longer be protected by formamide. The crystal growth inhibition in the Z direction was removed. Under thermal aging conditions, the nanosheets formed layered structures. Figure 19(A) shows the digital image of the aged sample after washing. The sample did not form a stable suspension. Instead, the sample precipitated out and settled on the bottom of the vial.

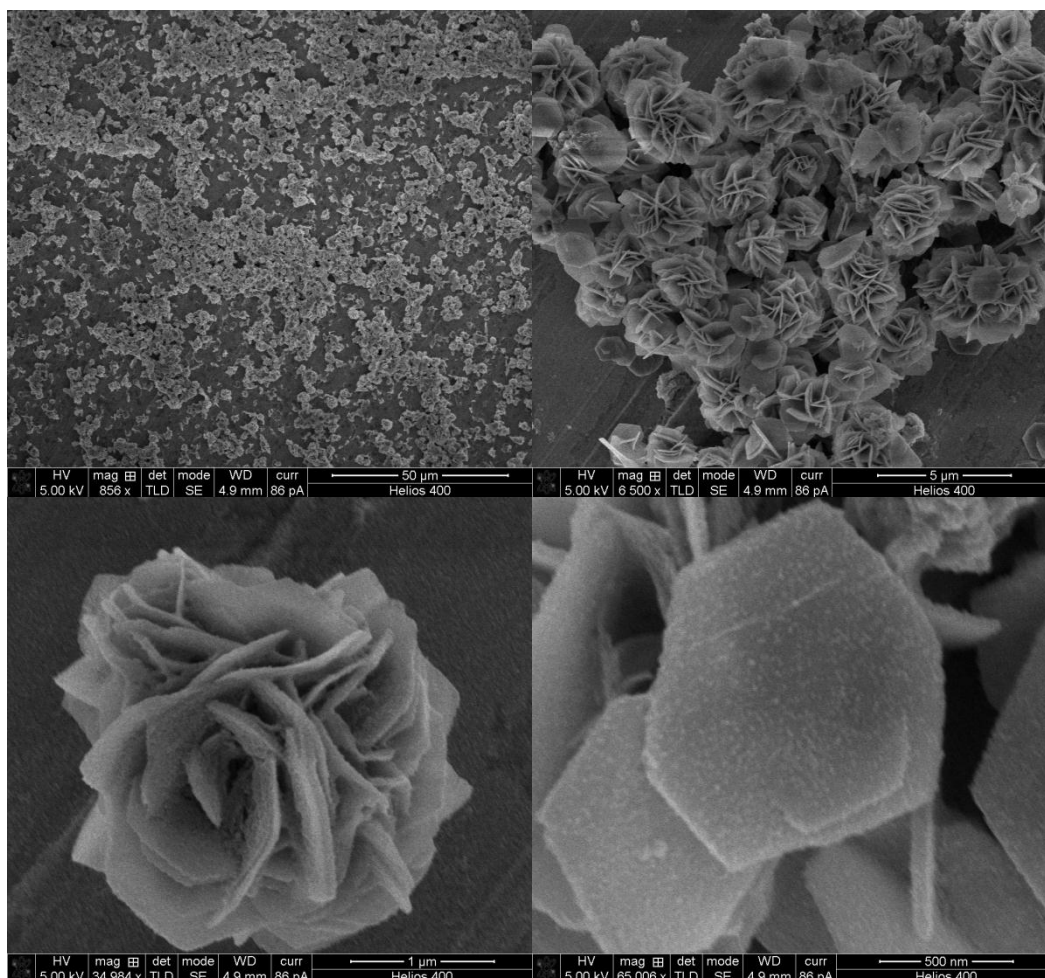


Figure 20. SEM images of Mg/Al-LDH nanosheets synthesized with 100 vol% formamide after aging.

4. Conclusions

The results shown above indicate that LDH nanosheets can be directly synthesized via the in situ synthesis method. Formamide molecules can act as an inhibitor during the in situ synthesis compromising the growth of LDH in the Z-direction at 23 vol% concentration. A relatively low concentration of formamide (5 and 10 vol%) may not effectively block the growth of LDH in the Z-direction resulting in LDH sheets with high crystallinity. These are very similar to the ones synthesized in the absence of formamide,

as evidenced by the TEM images. On the other hand, a high concentration of formamide (>50 vol%) produces LDH nanosheets with much lower crystallinity. At 100 vol% formamide, LDH growth was effectively inhibited producing amorphous like LDH. The conventional method to improve LDH crystallinity, aging, is however, not viable in our system because of the hydrolysis of formamide in strong base.

Further characterization, such as atomic force microscopy, is required to confirm the thickness of the LDH nanosheets. Further studies of the stabilization mechanism of LDH nanosheets in solution needs to be determined. The application of the directly synthesized LDH nanosheets to fabricate multifunctional nano-structured materials will be explored in the future studies.

References

1. Osada, M.; Sasaki, T., Two-Dimensional Dielectric Nanosheets: Novel Nanoelectronics From Nanocrystal Building Blocks. *Advanced Materials* **2012**, *24* (2), 210-228.
2. Novoselov, K. S.; Geim, A. K.; Morozov, S. V.; Jiang, D.; Zhang, Y.; Dubonos, S. V.; Grigorieva, I. V.; Firsov, A. A., Electric Field Effect in Atomically Thin Carbon Films. *Science* **2004**, *306*, 666-669.
3. Xu, Z. P.; Zhang, J.; Adebajo, M. O.; Zhang, H.; Zhou, C., Catalytic applications of layered double hydroxides and derivatives. *Applied Clay Science* **2011**, *53* (2), 139-150.
4. (a) Liu, Z.; Ma, R.; Osada, M.; Iyi, N.; Ebina, Y.; Takada, K.; Sasaki, T., Synthesis, Anion Exchange, and Delamination of Co-Al Layered Double Hydroxide. Assembly of the Exfoliated Nanosheet/Polyanion Composite Films and Magneto-Optical Studies. *Journal of the American Chemical Society* **2006**, *128* (14), 4872-4880; (b) Liu, Z.; Ma, R.; Ebina, Y.; Iyi, N.; Takada, K.; Sasaki, T., General Synthesis and Delamination of Highly Crystalline Transition-Metal-Bearing Layered Double Hydroxides. *Langmuir* **2006**, *23* (2), 861-867; (c) Li, L.; Ma, R.; Ebina, Y.; Iyi, N.; Sasaki, T., Positively Charged Nanosheets Derived via Total Delamination of Layered Double Hydroxides. *Chemistry of Materials* **2005**, *17* (17), 4386-4391; (d) Hibino, T., Delamination of Layered Double Hydroxides Containing Amino Acids. *Chemistry of Materials* **2004**, *16* (25), 5482-5488; (e) Adachi-Pagano, M.; Forano, C.; Besse, J.-P.,

Delamination of layered double hydroxides by use of surfactants. *Chemical Communications* **2000**, (1), 91-92.

5. Liu, Z.; Ma, R.; Osada, M.; Iyi, N.; Ebina, Y.; Takada, K.; Sasaki, T., Synthesis, Anion Exchange, and Delamination of Co–Al Layered Double Hydroxide: Assembly of the Exfoliated Nanosheet/Polyanion Composite Films and Magneto-Optical Studies. *Journal of the American Chemical Society* **2006**, 128 (14), 4872-4880.

6. Ma, R.; Liu, Z.; Li, L.; Iyi, N.; Sasaki, T., Exfoliating layered double hydroxides in formamide: a method to obtain positively charged nanosheets. *Journal of Materials Chemistry* **2006**, 16 (39), 3809-3813.

7. Hibino, T.; Yamashita, Y.; Kosuge, K.; Tsunashima, A., Decarbonation behavior of Mg-Al-CO₃ hydrotalcite-like compounds during heat treatment. *Clays and Clay Minerals* **1995**, 43 (4), 427-432.

8. Ma, S.; Wang, J.; Du, L.; Fan, C.; Sun, Y.; Sun, G.; Yang, X., Co-Assembly of LDH Nanosheets with Crown Ethers: Structural Transformation and Water-Adsorption Behavior. *European Journal of Inorganic Chemistry* **2013**, n/a-n/a.

9. Cavani, F.; TrifirÃ², F.; Vaccari, A., Hydrotalcite-type anionic clays: Preparation, properties and applications. *Catalysis Today* **1991**, 11 (2), 173-301.

10. Blumberger, J.; Ensing, B.; Klein, M. L., Formamide Hydrolysis in Alkaline Aqueous Solution: Insight from Ab Initio Metadynamics Calculations. *Angewandte Chemie International Edition* **2006**, 45 (18), 2893-2897.

CHAPTER III

IN SITU SYNTHESIS OF LDH/POLYELECTROLYTE INTERCALATION COMPOUNDS

1. Introduction

Intercalation of layered double hydroxides(LDHs) can be achieved by anion exchange,¹ the reconstruction of calcined LDH in the presence of target anion,² and the in situ growth of polymeric anions intercalated LDH.³ The in situ intercalation method has been achieved by Messersmith et al.,⁴ Oriakhi et al.,⁵ Whilton et al.,⁶ and Leroux et al.⁷ by precipitating different types of LDHs in the presence of polymers. It was suggested by Messersmith and coworkers⁴ that the incorporated PVA molecules promote the nucleation and growth of LDH layers. Thus, our attention was drawn to the idea of utilizing negatively charged polymers to guide the growth of LDH in the Z-direction. The previous in situ intercalations were performed using the titration method, which typically results in LDHs with a low crystallinity.⁸ Urea hydrolysis and hydrothermal conditions, which facilitate the crystallization of LDHs⁹ was adopted in this research. In this study, different weight percentages of two polyelectrolytes, poly(sodium 4-styrene-sulfonate) (PSSS) and poly(acrylic acid, sodium) (PAAS), were added to the synthesis of LDH to examine the effect of polyelectrolytes on the growth of LDH in the Z-direction. PSSS is a strong polyelectrolyte which fully dissociates in solution, thus, it will be fully charged.

On the other hand, PAAS is a weak polyelectrolyte, which will be partially charged as a function of the PH of the solution. Morphology and crystallinity changes of two polyelectrolytes intercalated LDH compounds are expected to be different.

2. Experimental

2.1 Materials

$\text{Mg}(\text{NO}_3)_2 \cdot 6\text{H}_2\text{O}$ (98%) was purchased from Alfa Aesar Co.. $\text{Al}(\text{NO}_3)_3 \cdot 9\text{H}_2\text{O}$ (99%) was obtained from Acros Organics Co. Poly(acrylic acid, sodium) (35 wt. %) and Poly(sodium 4-styrene-sulfonate) (30 wt. %) solution in water were obtained from Sigma-Aldrich.

2.2 Synthesis method

Hydrothermal synthesis of Mg4Al-LDH

Metal salts [$\text{Mg}(\text{NO}_3)_2$, $\text{Al}(\text{NO}_3)_3$] were mixed with 30 mL of D.I. water. The Mg:Al content was in a 4:1 molar ratio. Total metal ion concentration was 0.25 M. Urea was added to the metal salts solution at a molar ratio of (urea) : (total metal ion) = 4:1. The mixture was added to a Teflon liner hydrothermal reactor and heated at 100 °C for 24 hours.

Intercalation compounds synthesis:

We assume that the metal ions were completely converted into LDH.

Samples of LDH with PSSS(or PAAS) were in a weight ratio: 4:1, 2:1, 1:1 and 1:2 were synthesized using the hydrothermal method listed above.

2.3 Characterizations

FT-IR spectra were recorded on a Perkin Elmer Frontier FT-IR Spectrometer. The samples were mixed with KBr and compressed as pellets for characterization. The thermal properties of the samples were characterized by a thermogravimetric analyzer (TGA, TA Instruments model Q50) with an air atmosphere (40 mL/min) at a heating rate of 10 °C/min. X-ray diffraction (XRD) patterns were recorded on Bruker D8 diffractometer with Cu K α radiation ($\lambda = 1.5406 \text{ \AA}$, 40 kV, 30 mA). JEOL 4000EX at 400 kV for TEM imaging. Helios NanoLab 400 Dual Beam from FEI was employed for SEM imaging.

3. Results and Discussion

Previous reports^{3, 5} specified the importance of eliminating air during the intercalation of polyelectrolytes to exclude the incorporation of carbonate ions into LDH. In our study, the hydrolysis of urea will produce carbon dioxide. The exclusion of the carbon dioxide is not required in our study. The reactions proceeded in un-deaerated D.I. water. The synthesized intercalated compounds were characterized by X-ray diffraction and FT-IR to confirm the intercalation.

XRD analysis

Figure 21 shows the XRD patterns of LDH/PSSS intercalation compounds with different weight ratios. Compared with the pure LDH hydrothermally synthesized without any PSSS, the XRD pattern of LDH:PSSS=4:1 ratio sample shows two phases; the PSSS intercalated phase (19.8 \AA) and the carbonate phase of LDH (7.5 \AA).¹⁰ Two phases co-exist because the amount of polymer added is not sufficient to fully occupy the interlayer region of LDH. Additional anions are needed to compensate the layer charge of

LDH. Carbonate ion is well known as the preferred anion for LDH because of the favorable lattice stabilization enthalpy. It was stated that “attempted syntheses of the polymer-LDH nanocomposites in air always resulted in the carbonate form with no evidence of polymer incorporation.”⁵ Previous attempts to synthesize LDH with singly charged polymers were not successful. The success of our direct intercalation of polyelectrolyte into LDH in air can be ascribed to the large amount of polyelectrolyte used and the high pressure and high temperature during the synthesis. Increasing the amount of PSSS, decreased the amount of the carbonate LDH relative to PSSS intercalated LDH. At the weight ratio of LDH:PSSS=1:1, the peak of carbonate LDH completely disappeared. Only one type of LDH was shown in XRD pattern starting from the sample of LDH:PSSS=1:1, which indicates that the dominating interlayer ion was the polymer. Moreover, the first order peak broadened with increasing amounts of PSSS. The average d-spacing of the first order peak of the LDH:PSSS=1:1 and 1:2 is ca. 20.5 Å, which is similar to the data in the literature.^{5, 11} The details of XRD patterns for MgAl-LDH, PSSS/LDH and PAAS/LDH intercalation compounds are listed in Table 1.

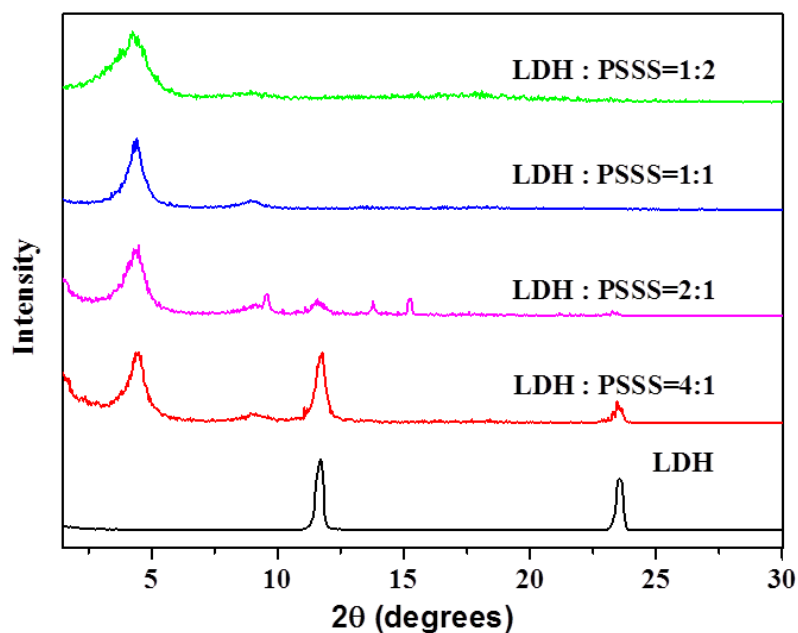


Figure 21. XRD patterns of LDH/PSSS intercalation compounds with different weight ratios of PSSS.

Figure 22 shows the XRD patterns of Mg/Al-LDH and LDH/PAAS intercalation compounds with different weight ratios of PAAS. The XRD patterns are different from the LDH/PSSS intercalation compounds shown in Figure 21. At the LDH/PAAS weight ratio of 4:1, the synthesized product does not show any sign of intercalation. Only the carbonate LDH phase is shown in the XRD pattern (see Table 1.), which can be ascribed to the weak polyelectrolyte effect. Increasing the amount of PAAS, the amount of carbonate LDH was decreased. At the weight ratio of LDH:PAAS = 1:1, no carbonate LDH is shown in the XRD pattern. Moreover, the diffraction peak of the product was very broad, which can also be ascribed to the weak polyelectrolyte effect.

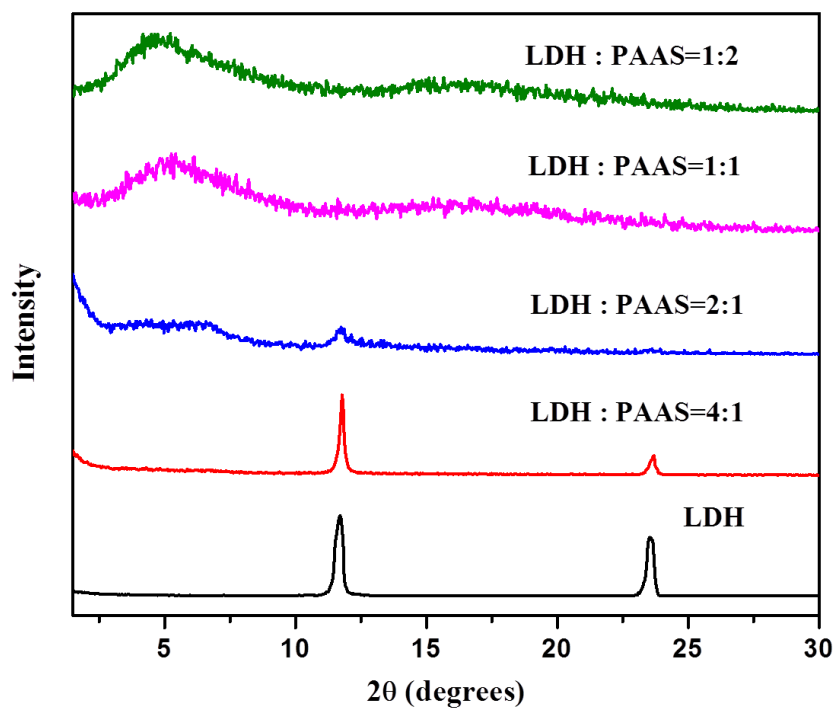


Figure 22. XRD patterns of LDH/PAAS intercalation compounds with different weight ratios of PAAS.

For LDH/PSSS intercalation compounds, the XRD patterns show that the intercalation compounds exhibit a close interlayer distance of ca. 20 Å, regardless of the amount of PSSS in the reaction. However, for the LDH/PAAS intercalation compounds, only the first order of the intercalation phase can be detected. Moreover, the intercalation phase is not manifested until LDH/PAAS=2:1 which all together were ascribed to the weak polyelectrolyte effect.

Table 1. XRD data for Mg/Al-LDH and polyelectrolyte intercalation compounds.

Sample	$d / \text{\AA}$			
	Intercalation Phase		CO_3^{2-} -LDH Phase	
	First order	Second order	First order	Second order
Mg/Al-LDH	–	–	7.5	3.8
LDH:PSSS				
4:1	19.8	9.8	7.5	3.8
2:1	20.0	10.0	7.6	3.8
1:1	20.2	9.9	–	–
1:2	20.3	10.1	–	–
LDH:PAAS				
4:1	–	–	7.5	3.8
2:1	14.0	–	7.5	3.8
1:1	17.3	–	–	–
2:1	19.0	–	–	–

IR analysis

The IR spectra of the carbonate LDH and polyelectrolyte intercalation compounds are shown in Figure 23 and 24. In Figure 23, different weight ratios of LDH/PSSS intercalation compounds are shown. The strong peak at 1370 cm^{-1} can be assigned to the stretching of C=O in CO_3^{2-} in the pristine LDH spectra.¹² In the IR spectra of the intercalation compounds, the sharp peak at 1040 cm^{-1} , the symmetric stretch, and broad peak at 1196 cm^{-1} , the asymmetric stretch, are the characteristic vibrations of sulfonate

R-SO_3^- from sulfonic acid.¹³ The intercalation of PSS^- into the interlayer space is confirmed by the presence of two absorptions at 1040 and 1196 cm^{-1} , even at a ratio of $\text{LDH}:\text{PSSS}=4:1$. With an increasing concentration of PSSS, the interlayer carbonate anion was gradually replaced by PSS^- . The gradual reduction of the carbonate absorption in the IR from $\text{LDH}:\text{PSSS}=4:1$ to $1:1$ is consistent with this hypothesis. No carbonate absorption peak was detected in the IR spectra of $\text{LDH}:\text{PSSS}=1:2$ which may indicate the complete replacement of carbonate ions by PSS^- .

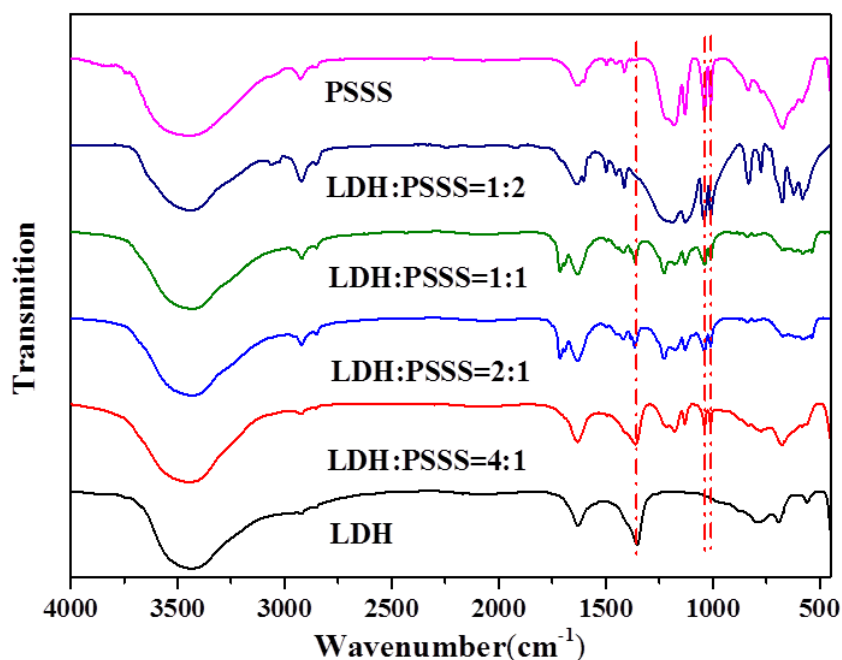


Figure 23. IR spectra of LDH/PSSS intercalation compounds with different weight ratios of PSSS.

Figure 24 shows the IR spectra of different weight ratios of LDH/PAAS intercalation compounds. The RCO_2^- characteristic IR absorptions in the intercalation compounds are at 1455 (symmetric RCO_2^- stretch) and 1566 cm^{-1} (asymmetric RCO_2^- stretch).¹⁴ In the IR spectra of the LDH/PAAS intercalation compounds, the presence of the two absorption

peaks appeared at LDH/PAAS=2:1 and maximize at the ratio of 1:2. This is different from the LDH/PSSS intercalation compounds, which show sign of PSS⁻ starting from LDH:PSSS=4:1 owing to the weak polyelectrolyte effect of PAAS. There is a strong carbonate absorption peak at 1370 cm⁻¹ in the LDH/PAAS=4:1 IR spectra, which indicates that the dominant interlayer ion in the LDH is still carbonate. This is consistent with the XRD patterns, which indicate no intercalation phase (Figure 22). With an increasing concentration of PAAS, the carbonate absorption intensity decreased and at LDH:PAAS=1:2, the carbonate absorption peak completely disappeared in the IR spectra. The IR spectra agree very well with the XRD patterns, both of which show that at LDH:PAAS=1:1 and 1:2, the polyelectrolyte is the dominant interlayer anion.

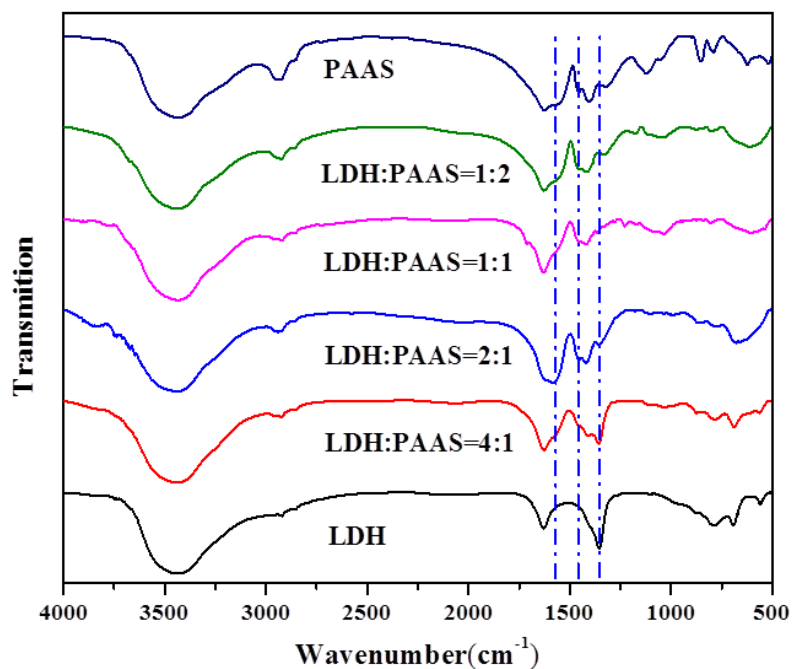


Figure 24. IR spectra of LDH/PAAS intercalation compounds with different weight ratios of PAAS.

TGA analysis

All samples were tested in the solid phase including the two polyelectrolytes. The two pure polyelectrolytes solution were dried in oven at 100 °C for a day. The solid intercalation compounds were ground into powders using a mortar and pestle.

Figure 25 shows the TGA analysis of carbonate LDH, LDH/PSSS intercalation compounds and PSSS. In the thermogram of the carbonate LDH, two transitions of weight loss are present. The first transition at ca. 70- 200 °C corresponds to 13.1% weight loss and the second one at ca. 200-330 °C corresponds to 7.7% weight loss. The two stages of weight loss can be attributed to the loss of surface water and interlayer water.⁸ The third stage at ca. 330- 520 °C corresponds to 16.3% weight loss, which was caused by the decomposition of carbonate and the dehydroxylation of the layers.⁸

In the thermo gram of the intercalation compound from LDH/PSSS=4:1, two transitions of weight loss are presented. The first transition is at ca. 70- 430 °C, owing to the elimination of absorbed surface water and interlayer water, which correspond to 17.8 % weight loss. The second stage is between ca. 430- 590 °C, which can be attributed to the dehydroxylation of the layers, loss of CO₂ from residue carbonate anions, and partial decomposition of the polyelectrolyte.⁵ Moreover, the PSSS IR spectra shows that the polyelectrolyte starts to decompose at ca.420 °C (Figure 26). The increased polymeric decomposition starting temperature of the intercalation compounds compared to neat PSSS indicated that the intercalated polymers were protected by the layers.

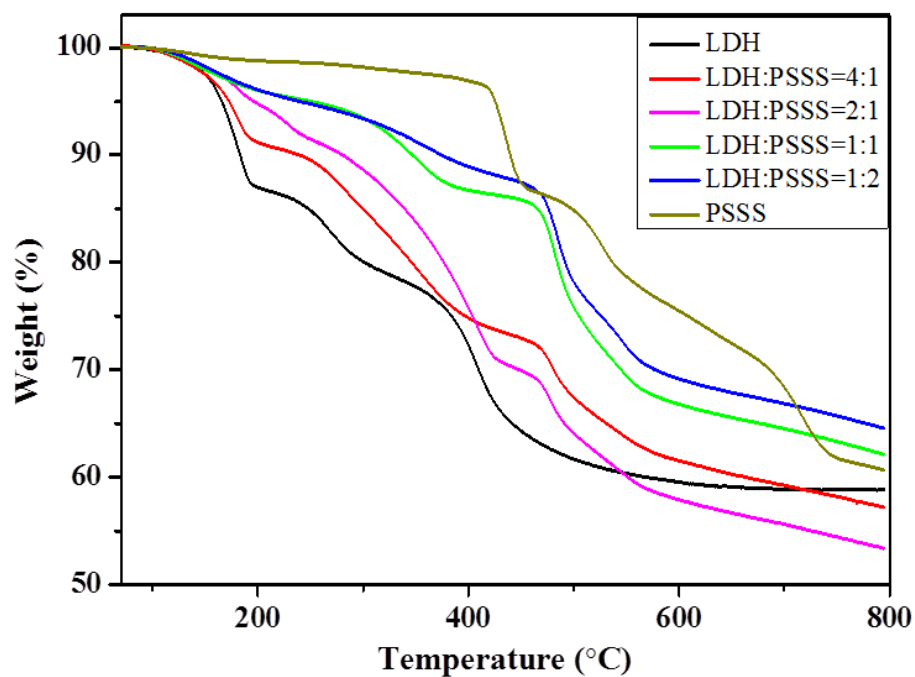


Figure 25. TGA profile of LDH/PSSS intercalation compounds with different weight ratios of PSSS.

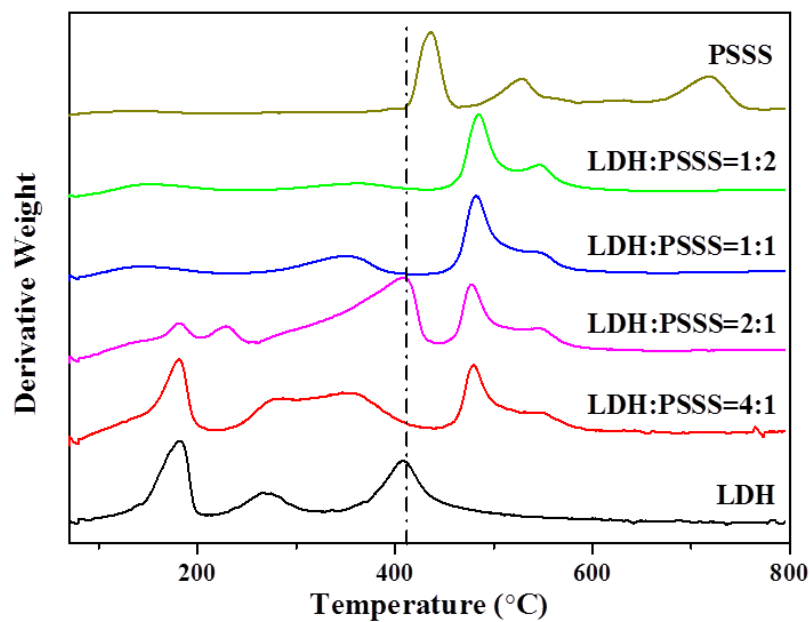


Figure 26. Derivative TGA profile of LDH/PSSS intercalation compounds with different weight ratios of PSSS.

The thermogravimetric analysis traces for the pristine LDH, LDH/PAAS intercalation compounds, and PAAS are shown in Figure 27. The pure PAAS shows two stages of weight loss corresponding to the decarboxylation¹⁵ of the PAAS at ca. 370 -390 °C and the decomposition of PAAS chain¹⁵ at ca. 390-530 °C. Similar to the LDH/PSSS intercalation compounds, as shown in Figure 28, all of the intercalation compounds exhibit a higher polymer decomposition starting temperature. This can again be attributed to the protection effect of LDH layers, and suggests the successful intercalation of polymers in the LDH layers.¹⁶

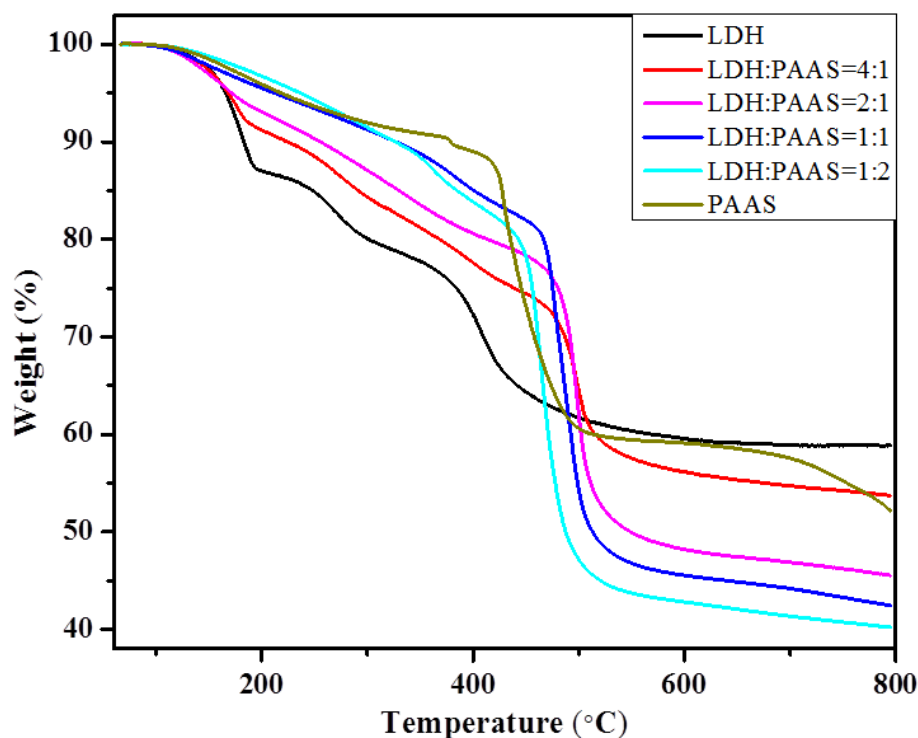


Figure 27. TGA profile of LDH/PAAS intercalation compounds with different weight ratios of PAAS.

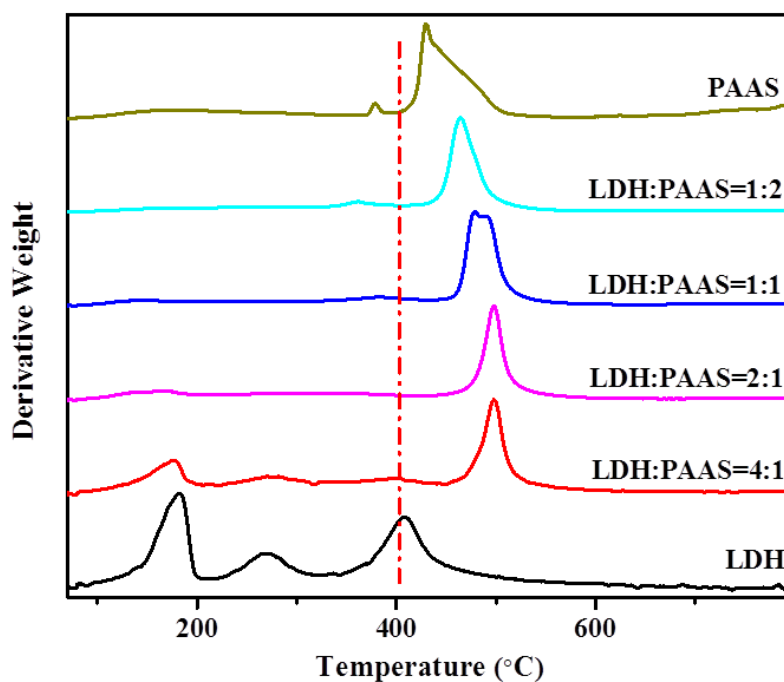


Figure 28. Derivative TGA profile of LDH/PAAS intercalation compounds with different weight ratios of PAAS.

SEM analysis

The control carbonate LDH synthesized under the same condition and the polyelectrolyte/LDH intercalation compounds were examined by the scanning electron microscope to examine the morphology of the samples. Figure 29 presents the typical LDH hexagonal layered morphology with SEM. The thickness of the LDH flakes is between 50-150 nm and the diameter is about 1-5 μm . Some of these platelets are aggregated into LDH piles.

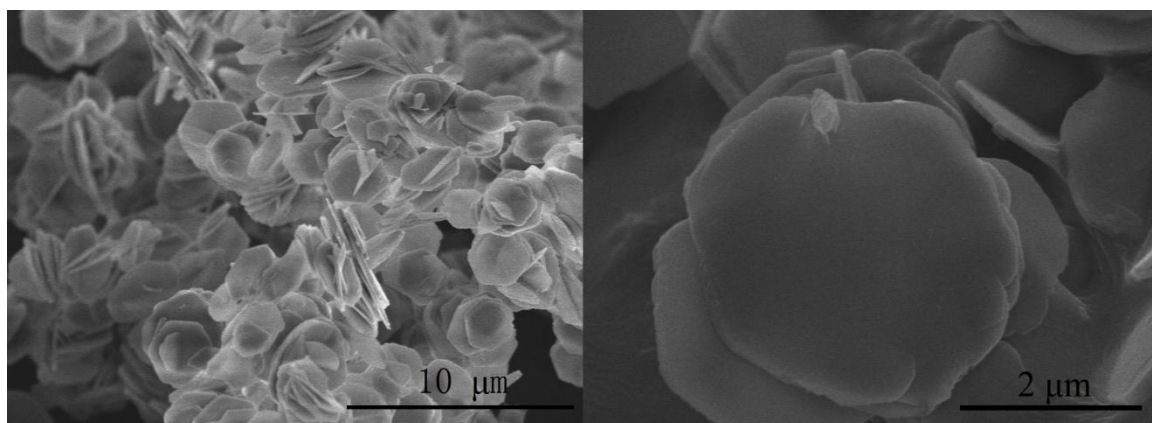


Figure 29. SEM images of the hydrothermally synthesized pristine LDH.

In contrast, the LDH/PSSS intercalation compounds show different microstructure from the pristine LDH (Figure 30). The intercalation compound LDH/PSSS=4:1 exhibited a rosette morphology. There is still platelet structure remaining that indicates the co-existence of the carbonate LDH and the intercalation compound. The LDH/PSSS=2:1 sample shows a similar morphology and a higher concentration of packed structure. With a further increased concentration of PSSS, the LDH/PSSS=1:1 sample showed few signs of platelet structure but more rosette-like structures and aggregates. As the PSSS concentration reached LDH/PSSS=1:2, only large aggregates can be observed which shows a thickness of dozens of microns (not shown in the image).

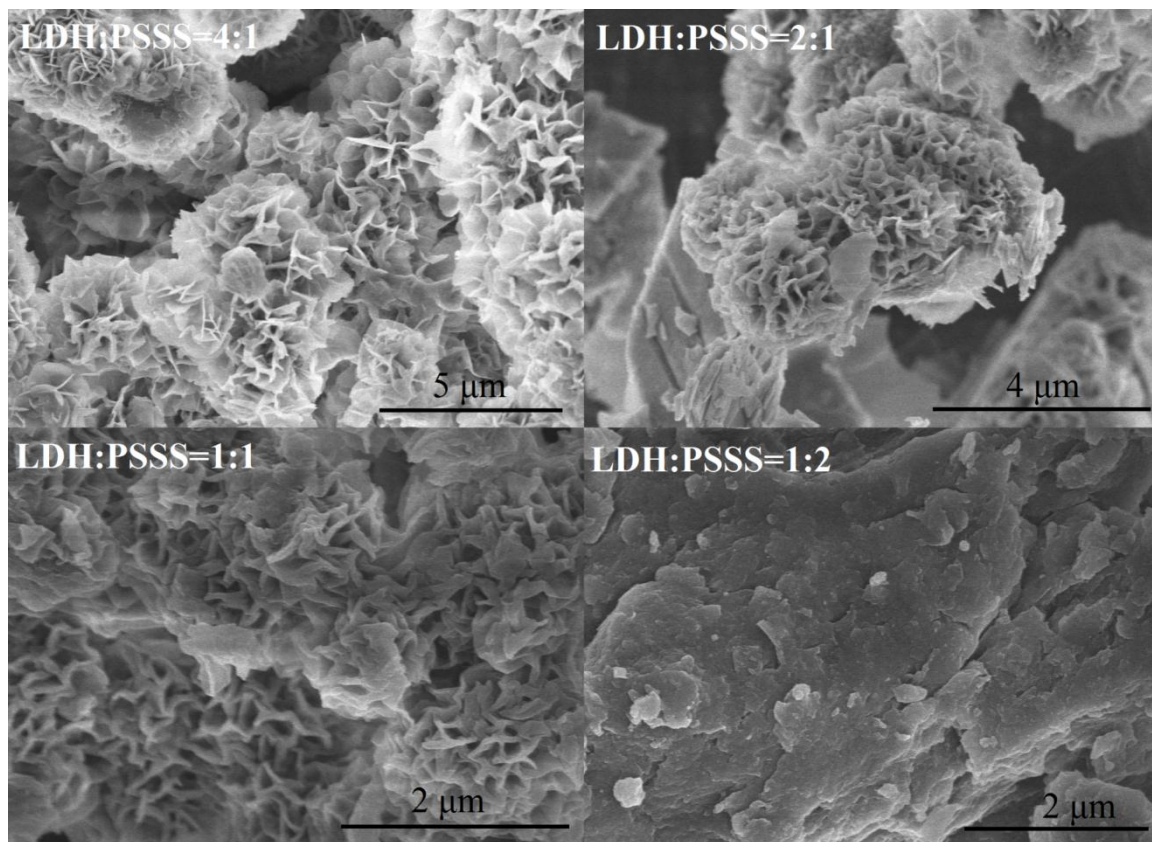


Figure 30. SEM images of LDH/PSSS intercalation compounds with different weight ratios of PSSS.

Similar to LDH/PSSS intercalation compounds, the SEM images (Figure 31) of LDH/PAAS=4:1 and 2:1 intercalation compounds showed the co-existence of a rosette like and platelet structure. However, the LDH/PAAS=1:1 intercalation compound showed a spherical structure along with large aggregates (not shown in the image). The SEM image of LDH/PAAS=1:2 shows only large aggregates with thickness of dozens of microns.

The SEM images show the effect of the presence of polyelectrolyte on the morphology of the formed layered compounds.

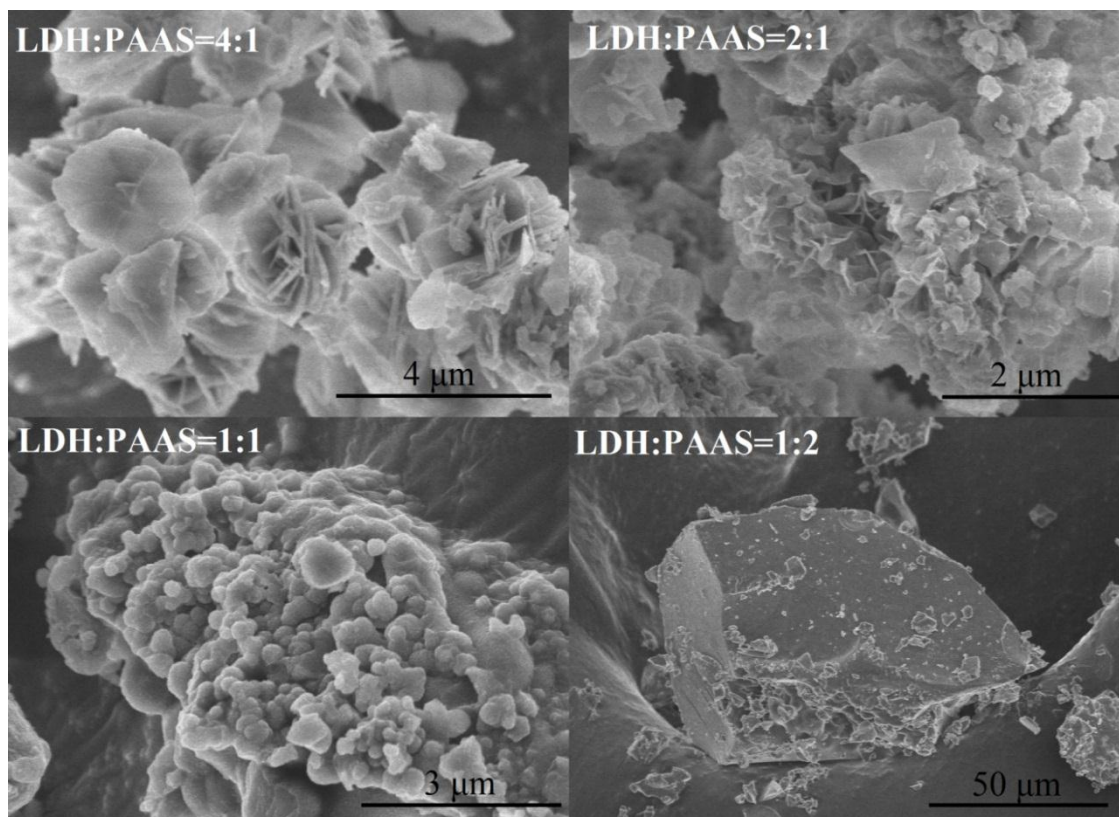


Figure 31. SEM images of LDH/PAAS intercalation compounds with different weight ratio of PAAS.

4. Conclusions

In this study, LDH and two LDH/polyelectrolyte intercalation compounds were prepared via an in situ hydrothermal method. The XRD and FT-IR data confirmed the successful intercalation. The thermal stability of the two polyelectrolytes was improved after intercalation, which is confirmed by the TGA. Moreover, the SEM images show that the presence of the polyelectrolytes had a significant effect on the morphology of the formed layered compounds.

In conclusion, the results show that the new in situ hydrothermal method is effective for the direct synthesis of LDH/polymer intercalation compounds.

References

1. (a) Kopka, H.; Beneke, K.; Lagaly, G., Anionic surfactants between double metal hydroxide layers. *Journal of Colloid and Interface Science* **1988**, *123* (2), 427-436; (b) Meyn, M.; Beneke, K.; Lagaly, G., Anion-exchange reactions of layered double hydroxides. *Inorganic Chemistry* **1990**, *29* (26), 5201-5207; (c) Carrado, K. A.; Forman, J. E.; Botto, R. E.; Winans, R. E., Incorporation of phthalocyanines by cationic and anionic clays via ion exchange and direct synthesis. *Chemistry of Materials* **1993**, *5* (4), 472-478; (d) Dutta, P. K.; Robins, D. S., Pyrene Sorption in Organic-Layered Double-Metal Hydroxides. *Langmuir* **1994**, *10* (6), 1851-1856.
2. (a) Chibwe, K.; Jones, W., Intercalation of organic and inorganic anions into layered double hydroxides. *Journal of the Chemical Society, Chemical Communications* **1989**, *0* (14), 926-927; (b) Tagaya, H.; Sato, S.; Morioka, H.; Kadokawa, J.; Karasu, M.; Chiba, K., Preferential intercalation of isomers of naphthalenecarboxylate ions into the interlayer of layered double hydroxides. *Chemistry of Materials* **1993**, *5* (10), 1431-1433.
3. Costa, F.; Saphiannikova, M.; Wagenknecht, U.; Heinrich, G., Layered Double Hydroxide Based Polymer Nanocomposites. In *Wax Crystal Control · Nanocomposites · Stimuli-Responsive Polymers*, Springer Berlin Heidelberg: **2008**, Vol. 210, pp 101-168.

4. Messersmith, P. B.; Stupp, S. I., High-Temperature Chemical and Microstructural Transformations of a Nanocomposite Organoceramic. *Chemistry of Materials* **1995**, 7 (3), 454-460.
5. Oriakhi, C. O.; Farr, I. V.; Lerner, M. M., Incorporation of poly(acrylic acid), poly(vinylsulfonate) and poly(styrenesulfonate) within layered double hydroxides. *Journal of Materials Chemistry* **1996**, 6 (1), 103-107.
6. Whilton, N. T.; Vickers, P. J.; Mann, S., Bioinorganic clays: synthesis and characterization of amino- and polyamino acid intercalated layered double hydroxides. *Journal of Materials Chemistry* **1997**, 7 (8), 1623-1629.
7. Leroux, F.; Aranda, P.; Besse, J.-P.; Ruiz-Hitzky, E., Intercalation of Poly(Ethylene Oxide) Derivatives into Layered Double Hydroxides. *European Journal of Inorganic Chemistry* **2003**, 2003 (6), 1242-1251.
8. Cavani, F.; TrifirÃ², F.; Vaccari, A., Hydrotalcite-type anionic clays: Preparation, properties and applications. *Catalysis Today* **1991**, 11 (2), 173-301.
9. Wang, J.; Li, D.; Yu, X.; Zhang, M.; Jing, X., Fabrication of layered double hydroxide spheres through urea hydrolysis and mechanisms involved in the formation. *Colloid Polym Sci* **2010**, 288 (14-15), 1411-1418.
10. Hibino, T.; Ohya, H., Synthesis of crystalline layered double hydroxides: Precipitation by using urea hydrolysis and subsequent hydrothermal reactions in aqueous solutions. *Applied Clay Science* **2009**, 45 (3), 123-132.

11. Vieille, L.; Taviot-Guého, C.; Besse, J.-P.; Leroux, F., Hydrocalumite and Its Polymer Derivatives. 2. Polymer Incorporation versus in Situ Polymerization of Styrene-4-sulfonate. *Chemistry of Materials* **2003**, *15* (23), 4369-4376.
12. del Arco, M.; Martin, C.; Martin, I.; Rives, V.; Trujillano, R., A FTIR spectroscopic study of surface acidity and basicity of mixed Mg, Al-oxides obtained by thermal decomposition of hydrotalcite. *Spectrochimica Acta Part A: Molecular Spectroscopy* **1993**, *49* (11), 1575-1582.
13. D. H. Williams and I. Fleming, Spectroscopic Methods in organic chemistry 3rd edn. *McGraw-Hill* **1980**, London, 64.
14. Fearheller Jr, W. R.; Katon, J. E., The vibrational spectra of acrylic acid and sodium acrylate. *Spectrochimica Acta Part A: Molecular Spectroscopy* **1967**, *23* (8), 2225-2232.
15. Garay, M. T.; Alava, C.; Rodriguez, M., Study of polymer–polymer complexes and blends of poly(N-isopropylacrylamide) with poly(carboxylic acid). 2. Poly(acrylic acid) and poly(methacrylic acid) partially neutralized. *Polymer* **2000**, *41* (15), 5799-5807.
16. (a) Rey, S.; Mérida-Robles, J.; Han, K.-S.; Guerlou-Demourgues, L.; Delmas, C.; Duguet, E., Acrylate intercalation and in situ polymerization in iron substituted nickel hydroxides. *Polymer International* **1999**, *48* (4), 277-282; (b) Berber, M. R.; Hafez, I. H.; Minagawa, K.; Tanaka, M.; Mori, T., An efficient strategy of managing irrigation water based on formulating highly absorbent polymer–inorganic clay composites. *Journal of Hydrology* **2012**, *470–471* (0), 193-200.

CHAPTER IV

SUMMARY AND FUTURE WORK

In this study, two methods were developed to tailor the growth of layered double hydroxides (LDHs) in the third dimension(Z direction): direct synthesis of single layer LDH nanosheets and LDH/polyelectrolyte layered intercalation compounds.

The synthesized LDH nanosheets exhibit apparent Tyndall effect in suspension. They were characterized by XRD and TEM. The characterization results we obtained so far have suggested that we have obtained very thin LDH nanosheets. However, further characterization, such as AFM and cryo-TEM must be conducted to verify that exact thickness of the nanosheets.

Meanwhile, LDH/polyelectrolyte layered intercalation compounds were synthesized through a new in situ intercalation method. To the best of our knowledge, this is the first report on in situ intercalation of LDHs in the presence of CO₂. Previous in situ intercalation methods were not successful in the presence of CO₂ using a titration method. The new method has been proved to be effective based on the XRD and FT-IR characterization of the synthesized intercalation compounds. Moreover, the SEM images confirmed the guidance effect of polyelectrolytes on the Z- direction growth of LDHs.

The above two related methods, one is based on inhibiting the growth of LDHs in the Z- direction, the other concentrates on improving the third dimension growth with the guidance of layer growth coordinators, have been proved to be effective as we expected.

Future work will focus on the further characterization of the as synthesized LDH nanosheets to confirm the layer thickness and their application in the fabrication of nano-structured materials. The hydrolysis of formamide in relationship to the aging chemistry will be confirmed. The study of macromolecular, inorganic, as well as other organic inhibitors/coordinators, which might function more effectively than formamide/polyelectrolytes, respectively is planned. In addition, the mechanism of the Z-direction growth of layered materials has not been fully defined, thus further more in-depth investigations are needed. Finally, the methods developed here will build a good foundation for tailoring the growth of 3-D materials with more sophisticated structures.

VITA

Jingfang Yu was born in Changsha, China, on January 07, 1988, the daughter of Guosheng Yu and Guozhong Xu. After completing her study at the 28th High school, Changsha, China, in 2007, she entered Xiangtan University. She received the degree of Bachelor of Engineering from Xiangtan University in June 2011. In August 2011, she entered the Graduate College of Texas State University-San Marcos.

Permanent E-mail Address: yujingfang2012@gmail.com

This thesis was typed by Jingfang Yu.